ISSN 0972-9984

International Journal of Ecology & Development

Volume 4 No. W06 Winter 2006

International Journal of Ecology &Development

ISSN 0972-9984

Editorial Board

International Journal of Ecology & Development

ISSN 0972-9984

Contents

Volume 4 **No. W06** **Winter 2006**

International Journal of Ecology & Development (IJED),
Winter 2006, Vol. 4, No. W06; Int. J. Ecol. Dev.; 1-22
ISSN 0972-9984; Copyright © 2006 IJED, ISDER

(Anticipated) Climate Change Impacts on Australia

P.Le C.F.Stewart[1] & SR Vemuri[2]

[1]School of Science and Primary Industries
Faculty of Education, Health and Science
Charles Darwin University
Darwin NT0909, Australia
philip.stewart@cdu.edu.au

[2]School of Law and Business
Faculty of Law, Business and Arts
Charles Darwin University
Darwin NT0909, Australia

ABSTRACT

This paper looks at the implications of climate change and the use of General Circulation Models, the risks involved and the uncertainties with predicting future climate outcomes with a focus on Australia and probable impacts on various industries and the biota of the Australian Continent. One thing we know for sure is that climate change is happening and the planet is getting warmer. Twelve of warmest years have occurred in the 1900's, 10 having occurred between 1987 and 1998. The top 300 metres of the sea surface temperature has increased, which may have catastrophic consequences for the planet if the conveyer belt system is changed or halted. With increased terrestrial temperatures diseases are now migrating into regions that they were not found in before. Evidence suggests that with the increased heating of the planet, energy availability will increase to drive extreme weather events, which could have a ripple effect throughout the Earth system with local, regional and global positive feedbacks feeding on each other, amplifying and accelerating warming. Due to the uncertainties in climate modeling we need to develop more accurate GCMs, which we need to link to the impacts they have on decision making, as predictions do not automatically transfer to the management of natural disasters as can be seen in the resent New Orleans Cyclone impact. As forecasting using GCMs only deals in probabilities, a cohesive and collaborative research approach to climate change is required to achieve success in assessing risk and uncertainty.

Keywords: Climate change, greenhouse gases, Biodiversity, General Circulation Models, Greenhouse warming.

1. Introduction

Human induced climate change is now beyond question, due to the overwhelming consensus among scientists that anthropogenic climate change is happening (Retallack *et al*, 1999, van Rood, 2000). Observations show that the Earth's annual global mean surface temperature has increased by approximately 0.6^{o}C between 1861 and 1997 (Bonan, 2002). Twelve of warmest years have occurred in the 1900's, 10 occurred between 1987 and 1998. This warming has occurred in two

distinct periods 1920 or 1940 and again in the 1970's to the present. The 1900's stand out as the warmest century, which had an unprecedented rate of warming (Mann *et al* 1998). There has also been an associated warming of the world's oceans by 0.3^{o}C in the top 300m since the mid 1950's (Levitus *et al*, 2000; Bonan, 2002). This surface and ocean warming makes the 1900's the warmest of the past five hundred years (Harris and Chapman, 2001). Bonan (2002) suggests that this warming is instrumental in reduced spring snow cover, northern hemisphere lakes and rivers freezing later in autumn and the thawing earlier in spring, melting of the Alpine glaciers, the Greenland ice sheet, permafrost, and shrinking of the artic ice pack. There has been a decrease in diurnal temperature range due to the increasing in daily minimum temperatures (Jones *et al*, 1999). It is expected that climate change will increase the frequency of extreme climate events (Bonan, 2002), resulting in changes in floods, droughts, and intense rainfall.

2. Global Temperatures

According to the IPCC (Intergovernmental Panel on Climate Change), average global temperatures have increased by 0.6^{o}C above the pre-industrial average. Further the IPCC predicts that if emissions continue to rise at present levels, by 2080 greenhouse gas concentrations may double (Retallack *et al*, 1999). This doubling of greenhouse gases may cause an average increase in temperature of between 2.5^{o}C and 4^{o}C over land masses and 3^{o}C to 4^{o}C over the Artic or Antarctic with substantial regional variations from the global average (Retallack *et al*, 1999). With higher temperatures there will be more energy availability to drive the planets climatic system, which in turn would cause more violent weather events. "Severe storms, floods, droughts, dust storms, sea surges, crumbling coastlines, saltwater intrusions of ground water, failing crops, dying forests, the inundation of low lying islands, and the spread of endemic disease such as malaria, dengue fever and schistosomiasis" (Retallack *et al,* 1999). There are correlations between warming and climatic catastrophe. For example, the increase of 1^{o}C mean annual temperature a metre below the surface in the northwest Canada and Alaska since 1989 (Retallack *et al*, 1999) which has resulted in the melting of the permafrost, causing the release of stored methane into the atmosphere and increasing greenhouse gases. As a result of the only 1^{o}C increase in annual mean temperature Retallack *et al* (1999) states

that “plants, insects, birds, and mammals, including disease are migrating further northward into regions too cold before". The average surface temperature has been increasing by 0.13^{o}C per decade and the lower stratosphere has been cooling by up to 0.5^{o}C per decade. Both pointing to a significant surface warming. “The only elements of uncertainty concern the precise effects global warming will have on the rest of the Earth’s climate stabilising systems, and the speed with which changes will occur.”(Retallack *et al*, 1999).

Bunyard (1999) states that climate change caused by CO_2 and other greenhouse gas levels in the atmosphere may have consequences on the positive feedbacks where these feedbacks become amplified, accelerating warming. A complication of positive feedbacks is the tendency for distinctly different processes to feed on each other in synergistic interactions. Presently about 7.5 billion tonnes of carbon is released into the atmosphere from the burning of fossil fuels each year (Bunyard, 1999). However projected predictions for carbon dioxide emissions by the United Kingdom Meteorology Office states that should they remain unmitigated, they will have a five fold increase in atmospheric carbon in 100 years to 1300ppm compared to pre-industrial 280ppm level and three times more than today’s 365ppm (see figure 1). Current ocean and land sinks presently remove on average over half the CO_2 emitted into the atmosphere by fossil fuel combustion. Models based on terrestrial sinks suggest that the sink strength will level off around the middle of the century and could drop after, at the same time the build-up of CO_2 will continue inexorably unless effectively abated.

3. Uncertainties and climate change

3.1 Global warming potential (GWP)

Global warming potential represents an attempt to develop a single index for quantitatively comparing the climatic affects of equal emissions of different greenhouse gases. With this attempt there are a number of significant uncertainties associated with global warming potentials, for example the direct radiative forcing of some gases and in particular the greenhouse gases, is still uncertain by up to 30%; some gases such as the halocarbons and methane have important indirect radiative forcing that are difficult to compute accurately; the atmospheric lifespan of some gases being compared to CO_2 are still uncertain; changes in climate could cause

important changes in the net rate of removal of CO_2 from the atmosphere, and this would alter the computed GWPs for all gases.

According to Danny Harvey (2000) the concept of GWP is an attempt to force the complexities of nature into a single number, which is not scientifically justifiable. Further it is more scientifically justifiable to compare climate change, and rates of change, for alternative emission scenarios using simple models (Harvey, 2000). Attention should be focused on the question of off setting the inevitable acceleration of warming as sulphur emissions are reduced, rather than the question of how much reduction in CO_2 emission can be achieved through reduced emissions of other gases. It has been the political process that has demanded a single number to inter compare different greenhouse gases. This is because current international agreements have ignored scientific reality by focusing on a collection of greenhouse gases rather than by framing gas-by-gas restrictions.

3.2 Surface warming

Surface warming is expected to increase to between 1.4^{o}C to 5.8^{o}C by 2100, which suggests a rate of warming about twice to ten times that observed during the 20th century, which was Approximately 0.6^{o}C and much faster than the average warming at the end of the last glaciation (Houghton *et al*, 2001).

3.3 Regional warming

Regional warming is associated with greater warming of the continental interiors and in the northern hemisphere, with lesser warming over the oceans and windward coastlines, with the least warming occurring over the southern ocean due to its capacity to transport surface heat into the deep ocean. Regional variability may see changes in precipitation and evaporation with either increases in or decline in either. Both variables have serious implications for the natural environment as well as the human socio-economical framework. Especially if warming is greater in the eastern Pacific than in the west leading to more El-Niño like mean state.

Precipitation is expected to increase as is evaporation by about 1% to 9% by 2100, depending on which climate model and scenario is used. Regional variation with increases over mid and high latitudes and Antarctic in winter may be expected. At the lower latitudes both an increase and decrease over land areas may be expected, which is supported by most global climate models (Houghton *et al*, 2000).

4. Risks

The Earth's geological history shows that the carbon dioxide levels once exceeded those of oxygen before the evolution of life, however with the evolution of photosynthetic plants, oxygen levels increased as carbon dioxide decreased (Gifford, 2003). CO_2 continued to decline until it reached the 180 to 300ppm range during the last 400 000 years of the current series of ice ages. During this period CO_2 concentration dropped to less than 200ppm at the peak of each ice advance and then climbed to almost 300ppm at the peak of each interglacial. During the last ice age about 18 000 years ago CO_2 concentrations were only about 180ppm. With the retreat of the ice the CO_2 concentration increased to about 280ppm by about two centuries ago. These changes in CO_2 concentration and climate had profound effects on ecosystems not directly affected by the ice cover (Gifford, 2003).

Turner *et al* (1991) suggests that there are five distinctive aspects of global environmental change with regard to risk analysis and management, which are; (i) caused by human activity, superimposed on physical or biochemical processes, which are always evolving and adjusting: (ii) Its effects are global in extent: (iii) It is characterised by rates of change in climate conditions that exceed presumed human capabilities to adjust to stressors: (iv) The scale of occurrence of its negative features are persistent as to be potentially irreversible: (v) Its remorselessness and cannot be avoided by the rich nations.

4.1 Predicting the outcomes

Predicting future climates and climatic outcomes is complex at best, however a method is needed to indicate predicted outcomes. Scenario driven approaches to impact studies is the method of choice, having achieved success in applying these

scenarios to drive models of changes (Steffen & Tyson, 2003). However scenario based approaches are limited due to their ability to only investigate impacts of single stressors. A second approach considers the outcomes of change with reference to a particular societal group, such as changes in food security or biodiversity. The focus being on the critical thresholds and driving factors for change (Steffen & Tyson, 2003) allowing for multiple and interaction stressors.

Past research has been on a single factor of change, whereas environmental changes are many, all changing at the same time. Therefore a single focused approach to predicting change is likely to fail, due to the lack of input of other impacts interacting and brought about by environmental changes. Steffen and Tyson (2003) state that sectorial science produced at local, landscape and regional scales are not sufficient, as a global system of global system science is needed. However the challenge to achieve this goal is exceptionally difficult, as it needs to include all players from developing and developed countries to achieve any success. Presently models used to assess the effects of global climate change are based on limited knowledge of the fundamental phenomena of climate and environmental change (Paté-Cornell, 1996). Not enough is known about all the processes of importance of climate change to include them in any quantitative forecast system as scientists are grossly underestimating the complexity of the interactions between the atmosphere, oceans, geosphere and biosphere. Models are used to generate scenarios of potential impacts of climate variability, changes, or extremes on ecosystems or on socioeconomic sectors (Glantz, 2003). Another method used is the historical or analogue approach which looks at how societies have responded to climate-related impacts in the past, where societal coping mechanisms if any are identified for use under present day circumstances (Glantz, 2003).

4.2 Probable impacts on economy

Most studies on climate change focus on impacts, mean temperature change and precipitation, but do not examine its welfare implications (Dalton, 1996). According to Dalton (1996), results show that serious bias predictions about welfare effects from global warming, with the possible underestimating of costs of climate change, could

develop due to the abstraction of climate variability. Underestimating these costs leads to policy recommendations with too little control on warming.

The implications for the economy due to climate change are enormous. The costs to the global insurance industry, agriculture and environment may be staggering with an increase in extreme weather events, desertification and sea level rise. The impacts on human health, medical costs to governments are other facts, which will have an impact on the global economy. However the costs to the global economy in the reduction of greenhouse emissions is costly. The estimated cost to the United States of reducing and stabilising one greenhouse gas CO_2 to 93% of the 1990's levels would cost between 2.4 million and 3.1 million jobs with a reduction in gross domestic product of between US$177 billion and US$318 billion. Whilst this cost is considerable, it is only a fraction of the cost to the global economy the world would have to spend each year to implement the Kyoto Protocol[1].

4.3 Probable impacts on tourism

Climate change has serious implications for the tourism industry worldwide and can be divided into two different types of climate impacts, direct and indirect impacts (Viner & Agnew 1999). Further tourism is an important contributor to the economies of most countries. The World Tourism Organisation report (1999) states that travel and tourism involved 625 million people internationally and generated $US 445 Billion in 1998 (Viner & Agnew 1999). Tourism is becoming increasingly vital in the economy of many countries and it is stated (Viner and Agnew, 1999) that the tourism industry involves more people and more money than any other industry on earth. Although this is arguable Table 1 below shows the top ten international holiday destinations.

The World Tourism Organisation predicted that international tourism would increase from 594 million in 1996 to 1600 million in 2020 (Viner and Agnew, 1999). This could mean an increase in revenue up to $US1.5 trillion by the year 2010. The direct impacts would influence the tourist as to when and where to visit, as the weather and season being dictating factors as to the objectives of the holiday destination. The

[1]Instant Expert's Guide to Global Warming: http://www.heartland.org/studies/ieguide.htm

indirect impacts arise as a result of the impact on the environment of a given location. The CSIRO (Australia) has carried out extensive modelling on the consequences in Australia of a failure to curtail global warming such as a possible accelerated coral bleaching, which could destroy part of the Great Barrier Reef by 2040, coastal flooding in New South Wales, and 66 percent less snow by 2030 and no snowfields in Australia by 2070, and the prediction of increased bushfires (Van Rood, 2000).

This has obvious serious consequences for the tourism industry that rely on these areas as tourist attractions. According to Viner and Agnew (1999), some resorts would become less of an attraction due to increased humidity or temperatures above comfort levels, whereas other resorts could develop into desired destinations because of the change in climate and weather. Viner and Agnew (1999) state “The most vulnerable tourist resorts and regions are a function of the likely magnitude and extent of the climate impact and the importance of tourism to the local economy.”

Table 1. Top World Destination 1996.

The table shows present top ten tourism destinations according to the World Tourism Organisation, with France being first preference and Canada in tenth place.

	Country	Arrivals (millions)
1.	France	61.5
2.	United States	44.8
3.	Spain	41.3
4.	Italy	32.9
5.	Britain	26.0
6.	China	22.8
7.	Mexico	21.4
8.	Hungary	20.7
9.	Poland	19.4
10.	Canada	17.4

Source: World Tourism Organisation.

4.4 Probable impacts on agriculture

According to Schimmelpfennig *et al* (1996), climate change is only one of several factors that may affect global agricultural production. Of interest is the

Intergovernmental Panel on Climate Change (IPCC) report of 1996 where it is estimated that climate change will cause temperatures to rise between 1.0 to 3.5 degrees Celsius. This was supported by the use of General Circulation Models (GCM) that the IPCC used to analyse climate change (Crosson 1997. The focus was on grain production with a focus on developed countries (DC) such as North America and Europe and on less developed countries (LDC) of Asia, Africa, and Latin America. According to Crosson (1997) grain was used as a proxy for all agricultural food production as it accounts for over half of all food calories consumed in the world. Three different GCMs, reflecting four different scenarios for estimating climate change impacts on grain were used as the IPCC sources (Crosson, 1997). The IPCC analyses of the four scenarios are summarised in Table 2.

Table 2: Estimated Percentage Grain Production Changes from Climate Change

Scenario	**World**	**Developed Countries**	**Developing Countries (Asia, Africa, Latin America)**
No offsetting effects considered	-11 to -20	-4 to -24	-14 to -16
Including CO_2 fertilization effect	-1 to -8	-4 to +11	-9 to -11
Including CO_2 fertilization and Modest farmer adaptation	0 to -5	+2 to +11	-9 to -13
Including CO_2 fertilization and more ambitious farmer adaptation	-2 to +1	+4 to +14	-6 to -7

According to Schimmelpfennig *et al* (1996) other resource problems are likely to be affected by climate change such as weeds, insects, and other agricultural pests may be redistributed. Studies have shown a poleward movement of the pest ranges (Schimmelpfennig *et al*, 1996). This has implications for production and costs thereof. With a warmer climate there may be an increased demand for water supply for crop growth and where this demand for water is not offset by increased precipitation or rainfall, 'climate change may further intensify the competition between growing urban, industrial, recreational, environmental, and agricultural users of water' (Schimmelpfennig *et al*, 1996).

Climate change threatens to increase hunger and malnutrition in the developing world, which is more vulnerable due to the importance of agriculture to their gross

domestic product, and the difficulties in making farm and regional level adjustments (Schimmelpfennig *et al*, 1996). Crosson (1997) states that a given percentage decline in production due to climate change would result in a greater percentage increase in prices, and vice versa for production increases. However, according to Schimmelpfennig *et al* (1996), the consequences of climate change on developing countries are relatively less important than other problems of agricultural development. This is based on four assumptions that the GCM used; give a reasonably accurate account of the anticipated changes that may occur on a global scale. The shortfall of this assumption is that the regional scale changes due to climate change are not known at this stage. The second assumption is that climate change will be linear in fashion: this being the gradual change without any extreme or severe changes in weather patterns (Schimmelpfennig *et al*, 1996). If this assumption is correct, it will give society time to adjust and adapt to the gradual changes.

However, according to climate records, the world's climate has changed in a short and chaotic fashion. This being the case, the consequences for agriculture may be more severe. Increasing extreme weather events and greater frequency of droughts and flooding can be associated with linear climate change. Schimmelpfennig *et al* (1996) claims that these possibilities are not picked up in scenarios of the IPCC.

4.5 Probable impacts on Oceania

The oceans, which cover over 70% of the world's surface, have sustained human life with the provision of fish and other seafood. The global population today still relies heavily on the sea for a living and more than US$500 billion of the world's economy is tied to ocean-based industries such as coastal tourism and shipping (WWF, 1999). However, the most important issue is that the oceans act to regulate the global climate through the absorption, storage and transfer of energy, and to ensure that a constant flow of nutrients are cycled throughout the biosphere. According to the World Wildlife Fund (WWF) Climate Change Campaign (1999), there is no doubt that the world is getting warmer. Examination of rings from trees and ice cores drilled into Antarctica, it has been determined that the past decade was the warmest in more than four centuries (as stated above) and that the current rate of warming is

unprecedented in at least 10,000 years. This warming is in part by emissions of greenhouse gases from fossil fuel use.

4.5.1 Implications for the thermohaline circulation.

Warming of the world's oceans provides the strongest evidence of global warming, and, more importantly, it appears to be affecting ocean conditions themselves (WWF.[b] 1999). One consequence could be more severe hurricanes. Therefore global warming could wreak greater havoc on ocean life than was first originally thought. The oceanic circulation, which is driven by a complex system of currents including the driving force of the deepwater movement, the thermohaline circulation or as it is sometimes called the ocean conveyer belt (Figure 1) is responsible for bringing oxygen to the deepest parts of the ocean, and for bringing warmer waters from the tropics towards the poles. The warmth of the water being carried into the northern Atlantic Ocean enhances its evaporation, which in turn, increases the waters saltiness and its density. The water then cools and sinks, forming the North Atlantic deep water (NADW) which forms a current flowing southward in the Atlantic Ocean, around Africa, and into the Indian and Pacific Oceans, where it mixes and slowly moves to the surface (Smith and Dukowicz 1993). This water near the surface flows back through the Pacific and Indian Oceans and north in the Atlantic Ocean, completing the global conveyer belt.

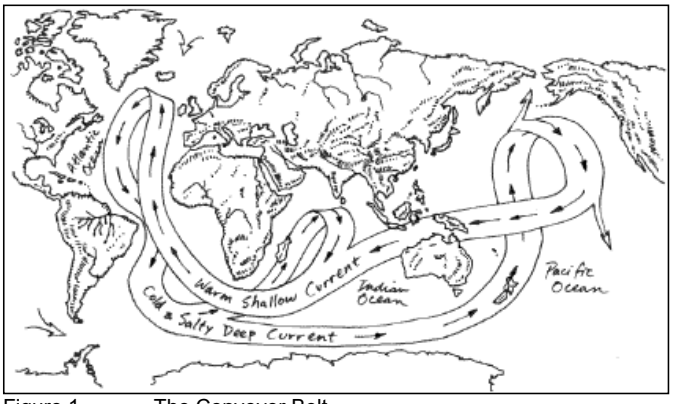

Figure 1. The Conveyer Belt
The Conveyer Belt is responsible for the transportation of heat energy from the tropics to the higher latitudes.

The conveyer belt mechanism depends on sinking cold water in polar regions, thereby triggering the global thermohaline circulation (Smith and Dukowicz 1993). According to the WWF (1999), global warming could alter the functioning of the conveyer belt in two ways; warmer water is less dense so any warming near the poles will reduce the downward flow. Freshwater is less dense than seawater, therefore the melting of the ice caps and polar glaciers would tend to reinforce the blockage of the system. The shutting down to the conveyer belt would have disastrous consequences for marine life and could induce a colder climate to Western Europe and the north Atlantic, as the warm Gulf Stream is interrupted (WWF, 1999). The density difference of the seawater determines the strength of the conveyer belt circulation, and any change in density differences due to climate change may lead to a weakening of the ocean current, which may result in a climate in north-western Europe, with more than 6 months of snow every year (Vellinga and van Verseveld, 2000).

4.5.2 Climate and the ocean

The ocean is a major component of the climate system and transports heat from the tropics to the polar regions in comparable amounts to that transported by the atmosphere (Smith and Dukowicz, 1993). Of importance is the ability of the ocean to act as a “thermal flywheel”, whereby it moderates changes that occur in the atmosphere (Smith and Dukowicz, 1993). It has been stated that the oceans, by sequestering heat trapped by greenhouse gases such as carbon dioxide and methane, could be delaying the onset of global warming due to human activities. According to Smith and Dukowicz (1993) paleoclimatic data and computer simulations both suggest that shifts in ocean-circulation patterns are associated with changes in climate. The conveyer belt system is a global scale circulation pattern and is driven by thermohaline effects (Smith and Dukowicz, 1993).

The El Niño Southern Oscillation phenomena, has profound implications for Agriculture, forests, precipitation, water resources, human health and society in general (Trenberth, 1996; Vellinga *et al*, 2000). According to Barsugli *et al* (1999), large scale weather events such as the January 1998 ice storm in the northern United States and the February 1998 rains in central and southern California may be

attributed to the 1997 – 98 El Niño. There have been more occurrences of El Niño's since 1975, and the duration of the 1990 – 95 El Niño was the longest on record (Vellinga *et al*, 2000). Daly (2003) states that "It has been found that the cyclic warming and cooling of the eastern and central Pacific leaves it's distinctive fingerprint on sea level pressure. In particular, when the pressure measured at Darwin is compared with that measured at Tahiti, the difference between the two can be used to generate an "index" number (Figure 2). When there is a positive number, we have a La-Niña (or ocean cooling), but when the number is negative we have an El-Niño".

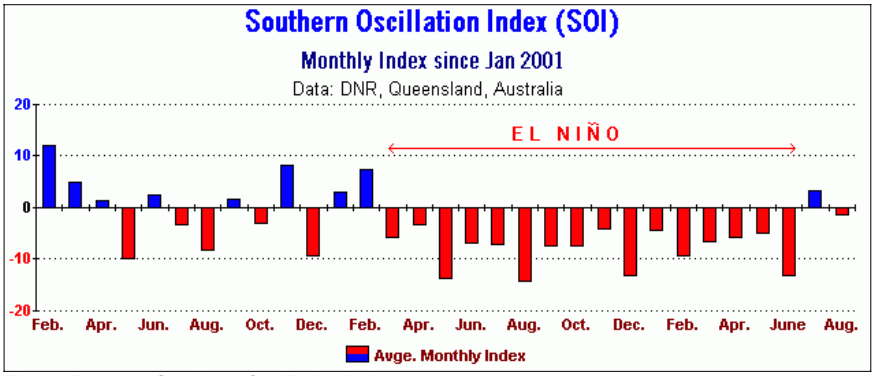

Figure 2. Southern Oscillation Index
The negative index for months from March to June shows an El Niño event for 2002. *Source*: Daly, J.L. (2003)[2]

The warming of the eastern tropical Pacific over the last decade, according to Knutson *et al* (1998), is likely due to a sustained thermal forcing, caused by increased greenhouse gases in the atmosphere. This suggests that human-induced climate change may in part be responsible for the extreme character of the El Niño-related weather over the past few years.

The North Atlantic Oscillation (NAO) is driven by a pressure difference between Iceland, and low-pressure area and a high-pressure area near the Azores, and is the dominant pattern of the wintertime atmospheric circulation of the North Atlantic. Over the past 30 years there has been an increase in the NAO index and since 1980 the NAO has remained positive (positive values of the NAO index indicate above average westerlies over the middle latitudes, which is related to pressure anomalies

[2] http://www.vision.net.au/~daly/elnino.htm

in this region). However, according to Vellinga *et al* (2000), no specific extreme weather event can be linked directly to climate change at present.

The observed warming of the Earth's surface does trigger changes in the frequency distribution of existing modes of climate variability, such as the NAO (Corti *et al*, *1999*). Further, the NASA Goddard Institute for Space Studies General Circulation Model (GCM) has shown that the increase in surface winds and continental surface temperatures of the Northern Hemisphere are the result of increased greenhouse gases (Vellinga *et al*, 2000). Shindell *et al* (1999) states that the comparison of various models indicates that surface changes are largely driven by the effect of greenhouse gases on the stratosphere.

In addition to the impacts on the NAO and El Niño by anthropogenic climate change factors, there has been a global increase in diseases affecting marine organisms. The increase in diseases has resulted in dramatic shifts in community structure, (Harvell *et al*, 2000). In addition to diseases there has been a reported increase in frequency of toxic algal blooms in the last decade. Further research work is needed to identify whether or not there is a correlation between global warming and the increase in marine diseases.

5. Impacts on Australia

Australia's climate is strongly influence by the surrounding oceans and the climatic features include tropical cyclones and monsoons in regions northern and mid-latitude storm systems in the south; and the El Niño-Southern Oscillation (ENSO) phenomenon (IPCC 2000). In 1998 Australia recorded its highest mean annual temperature since 1910, of 22.54 C, which was 0.73 C higher than the average for 1961 to 1990 reference period (Bureau of Meteorology, 1999). The mean minimum temperature during this period was 16.20 C, which was 1.03 C above the 1961 – 1990 average, well above the previous highest departure of 0.88 C set in 1973 (Bureau of Meteorology, 1999).

There is a trend where the mean annual temperature in Australia is increasing and much of the increase has been since the 1970s (Climag, 2000). Further minimum

temperatures have been warming up more than the maximum, particularly the eastern side of Australia. According to the IPCC special report (2000) on The Regional Impacts of Climate Change An Assessment of Vulnerability, night time temperatures have risen faster than the daytime temperatures. Sea levels have risen by about 20 mm per decade over the past 50 years (IPCC, 2000). The largest contribution to the record mean temperature has came from the warmer than usual minimum temperatures in the northern half of the continent, although some southern parts were actually cooler than normal for 1998 (Bureau of Meteorology, 1999).

The CSIRO has produced scenarios for 2030 and 2070, where temperature increases of up 0.3 to 1.4^{o}C and rainfall changes of up to 10% (IPCC. 2000, Ecos, 1999). The projected changes for 2070 are twice that of the 2030 scenario (IPCC, 2000). Further according to Science News (1995 vol.148 Issue 16, p255) a study of records of north eastern Australia found an increase in the strength of heavy precipitation during the 20th century. With an increase in sea-surface temperatures along Australian coastlines cyclones may move further south, combined with strong onshore winds, may rise sea level at its centre by a metre. (O'Neill, 1999).

5.1 Impact on Australian Agriculture

Climate plays a major role in yield, year-to-year variability and regional patterns of pastoral agricultural production in Australia (Campbell *et al*, 1996). It is understood that future changes in climate and atmospheric carbon dioxide concentration are expected to have both positive and negative impacts on pastoral agricultural production (Campbell 1994. Campbell, *et al* 1996). No comprehensive impact analysis has been conducted for the whole of Australia, however there have been regional analyses for areas such as Queensland (Weston *et a.*, 1981; McKeon *et al*, 1988; Campbell *et al*, 1996).

5.2 Impact on coastal regions and Islands of Australia

It has been predicted that sea-levels could rise between 25cm and 80cm by the year 2100, with the IPCC estimating a 50cm rise (Moore, *et a,.* 1996; IPCC, 1996). This may result in inundation of coasts, increased coastal erosion, flooding, salt-water

intrusion and the loss of coastal wetlands (IPCC, 1996). According to (Moore *et al*, 1996), if sea-level rise is accompanied by an increased frequency or intensity of extreme weather events such as cyclonic surges, then some Australian urban areas will be at risk. (IPCC, 1996). Australia's northern and eastern coasts are likely to be mostly affected by these extreme weather events and storm surges (Moore *et la*, 1996).

At present the current global rate of sea-level rise is observed to be 1.8 mm per year (Douglas, 1991), which may modify the expected surface warming on land due to changes in the ocean surface and subsurface temperatures. The rate of sea-level rise for Australia has been computed as 1.07 mm per year (Salinger *et al* ,1996), however there is great variability in sea-level trends, which is argued that a few decades (Douglas, 1991) of tidal gauge data are of little use for determining global trends.

Tidal channels have expanded over the last few decades in the freshwater floodplains of the lower Murray River and macrotidal systems in the Northern Territory (Chappell *et al*, 1996). However it is not known to what extent sea-level rise has had an impact as feral buffaloes have been implicated in the formation of new channels (Knighton *et al*, 1992; Chappell *et a,.* 1996). Chappell *et al* (1996) states, creek networks will become more extensive if sea-level continue to rise, and that freshwater communities will be killed by invading brackish waters. Assessment of potential coastal impacts due to climate change have been carried out in Australia (Cocks *et al*, 1988; Thom, 1989; Chappell *et al*, 1996; Kay *et al*, 1996). These impacts are expected to vary considerably according to regional and local environmental conditions.

5.3 Impacts on Australian biota

Australia's biota may be facing a greater rate of long-term change, and will have to respond to highly altered landscapes, which have become fragmented by agricultural and urban development.(IPCC, 2000). It is stated that migration may be an alternative for some biota (Mitchell and Williams, 1996), as some ecosystems are expected to shift, and having differential rates of migration, cause a change in

abundance and distribution of species (IPCC, 2000). According to Peters (1992), alternate species interactions may eliminate formerly successful species even if the climate remains within their physiological tolerances.

Due to slow reproduction rates or limited seed dispersal mechanisms, some species will be slow to migrate, this will allow other more tolerant species with better capacity for dispersal and establishment to increase (IPCC, 1996; IPCC, 2000). Many species will be able to adapt, it is expected that biodiversity will reduce in individual ecosystems due to climate change (IPCC, 1996; WG II, Section 1.3.6). Migration to higher altitude or elevations (decrease in air temperature with increase in altitude; 1.98^{o}C per thousand foot increase in elevation), is not an option in most parts of Australia due to its mainly flat expanses. Central Australia limits migration due to deserts and southward migration is restricted by the oceans for terrestrial biota (IPCC, 2000). Morton *et al* (1995) states that the survival of vulnerable species in refugia and their expansion into adjacent areas will be limited if there is an increase in frequency or intensity of climatic extremes, which will inhibit their migration. The ability of an organism to migrate will depend on its strength of dispersal. Further climate is a key factor influencing the broadscale geographical distribution of plants (Ficher *et al*, 2001), which may prevent the migration of an organism due to habitat modification or change. This is supported by Gioia and Pigott (2000), where predictors for distribution were found to be climatic.

According to the CSIRO (1999) drier winters are to be expected by the year 2030 accompanied by extra rains in November to April in the northwest with a 5 – 20% increase in rain for every 1^{o}C in increase in global temperature, with a 0 – 10% in the inland southern and eastern parts of Australia. This may be accompanied by less rain during the period from May to October, especially in the southern inland areas. There may be up to 10% decrease in rain in Western Australia, parts of South Australia and the Northern Territory. With this evaporation is expected to rise between 2 – 4% and relative humidity may increase or decrease by up to 4% depending on whether the rainfall increases or decreases for every degree C of global warming.

According to Mitchell *et al* (1996), increase in temperatures will not be spatially or seasonally uniform (Salinger *et al*. 1996), with greater impacts on minimum

temperatures than on maximum temperatures, such as a proportionately lesser cooling at night. This change in day/night temperature balance may also affect plants with respiration becoming more active and a need for compensation by daytime photosynthesis (Mitchell *et al*, 1996).

6. Conclusion

One thing that is certain is that the planet is getting hotter and is experiencing unprecedented environmental change. With increased emissions of CO_2, aerosols and halocarbons, increased land clearing for agriculture and suburban development, deforestation and an exponential population growth (there are more people alive today than have ever died), never in the history of the Earth has life been so threatened by risk and uncertainty due to environmental change. Evidence suggests that with the increased heating of the planet, energy availability will increase to drive extreme weather events, which could have a ripple effect throughout the Earth system with local, regional and global positive feedbacks feeding on each other, amplifying and accelerating warming.

Presently science lacks the ability and technology to predict with any certainty climate change and its associated impacts on the humans or the natural environment. Hedging ones bets being the preferred route to address emission abatement of greenhouse gases. The focus has been on single gas emission abatement scenario, which has obvious flaws with serious shortcomings and implications for the natural and human environment. The dynamics and interactive phenomena of gas emissions and especially the greenhouse gases are not taken into account. Risk management needs to be addressed from a global system of global system science. A more multi-level and dynamic approach is required, which investigates positive and negative feedbacks on a global level so as to avoid, if possible, any risks or uncertainty in future. Even with a global system of science in place, uncertainty will remain due to the variability in the climate/Earth systems interactions and feedbacks, to make any accurate predictions.

Not only do we need better and more accurate GCMs, we also need to link these model results to the impacts they have on decision making, as predictions do not

automatically transfer to the management of natural disasters as can be seen in the resent New Orleans Cyclone impact. Forecasting using GCMs will only deal in probabilities. A cohesive and collaborative research approach to climate change is required to achieve success in assessing risk and uncertainty, until such is achieved we will continue to be "surprised".

References

Bonan, G. 2002. *Ecological Climatology Concepts and applications*. Cambridge University Press. Cambridge. Pp 89 – 128.

Bunyard P.1999. How Climate Could Spiral Out of Control. *The Ecologist*. Vol 29 No 2.

Bunyard 2000. Fiddling While the Climate Burns. *The Ecologist* v30 i2 p48.

Bureau of Mereorology 1999. Record Warm Year for Australia in 1998. Media release issued 5th January .

Barsugli, J.J., Whitaker, J.S., Loughe, A.F., Sardeshmukh, P.D., and Toth, Z. 1999. The Effect of the 1997/98 El Niño on individual large-scale weather events. *Bulletin of the American Meteorological Society* 80(7).

Climag 2000. Climate – A never Trending Story? (Ed) White, B. Issue 3, March

Campbell, B.D. (1994). The current status of climate change research in relation to pastoral agriculture in New Zealand. National Science Strategy Committee for Climate Change, Information Series No. 7. The Royal Society of New Zealand, Wellington.

Crosson, P. 1997. Impacts of Climate Change on Agriculture. *Climate Issues Brief* No 4.

CSIRO. 1999. Future change in Australian Rangelands.(Eds) Stafford Smith, M. and Milligan, A. Dept Environment, Sport and Territories.

Campbell, B.D., McKeon, G.M., Gifford, R.M., Clark, H., Stafford Smith, D.M., Newton, P.C.D. and Lutze, J.L. (1996). Impacts of atmospheric composition and climate change on temperate and tropical pastoral Agriculture. In *Greenhouse: Coping with Climate Change,* Bouma, W.J., Pearman, G.I., and Manning, M.R. (eds), CSIRO `Publishing, Melbourne, pp. 171 – 189.

Chappell, J., Cowell, P.J., Woodroffe, C.D., and Eliot, I.G. 1996. *Coastal Impacts of `Enhanced Greenhouse Climate Change in Australia: Implications for coal use*. `Bouma, W.J., Pearman, G.I., and Manning, M.R., (eds), CSIRO Publishing, `Melbourne, pp. 220 – 234.

Corti, S., Molten, F. and Palmer, T.N. 1999. Signature of recent climate change in frequencies of natural atmospheric circulation regimes. *Nature* 398: 799-802.

Dalton, M. 1996: The Welfare Bias from Omitting Climatic Variability in Economic Studies of Global Warming. *Journal of Environmental Economics and Management* 33, 221–239 Article No. EE971000.

Daly, J.L. 2003. *The El-Niño Southern Oscillation (ENSO).* http://www.vision.net.au/~daly/elnino. htm

Danny Harvey, L.D. 2000. *Climate and Global Environmental Change*. Prentice Hall. Essex. Pp 205 – 207.

Douglas, D.C. 1991. Global Sea Level Rise. *Journal of Geophysical Research* 96 C4, 6981– 6992. Ecos Apr-Jun 1999 Issue 99, p23.

Ficher, J.D. Lindenmayer, H. A. Nix, J. L. Stein and J. A. Stein 2001. Climate and animal distribution: a climatic analysis of the Australian marsupial *Trichosurus caninus Journal of Biogeography*, 28, 293 – 304.

Gifford, R. 2003. Global Climate Change. In *Ecology an Australian Perspective.* Attiwill, P. & Wilson, B. (eds) Oxford University Press. Oxford. Pp 489 – 504 .

Glantz, M.H. 2003. *Climate Affairs. A primer.* Island Press. Washington. Pp 214 – 238.

Gioia, P and Pigott, J.P. 2000. Biodiversity assessment: a case study in predicting richness from the potential distributions of plant species in the forests of south-western Australia. *Journal of Biogeography*, 27, 1065 – 1078.

Harris, R.N., and Chapman, D.S. 2001. Mid-latitude (30o – 60o N) climatic warming inferred by combining borehole temperatures with surface air temperatures. *Geophysical Research Letters*. 28: Pp 747 – 750.

Harvell, C.D., Kim, K., Burkholder, J.M., Colwell, R.R., Epstein,P.R., Grimes, D.J., Hofmann, E.E., Lipp, E.K., Osterhaus, A.D.M.E., Overstreet, R.M., Porter, J.W., Smith, G.W., and Vasta, G.R. 2000. Emerging Marine Diseases—Climate Change and Anthropogenic Factors. (frequency and number of marine diseases has increased). *Science*, v285 i5433 p1505.

Houghton, J.T., Ding, Y., Griggs, D.J., Noguer, M., van der Linden, P.J., Xiaosu, D., Maskell, K., and Johnson, C.A. 2001. *Climate Change 2001: The Scientific Basis – Contribution of Working Group I to the Third Assessment Report of the Intergovernmental Panel on Climate Change* (IPCC). Cambridge University Press.

IPCC, International Panel on Climate Change (1996). Working Group II, Second Assessment Report, Cambridge University Press, Cambridge, UK.

IPCC: Intergovernmental Panel on Climate Change. 2000. *Special Report on The Regionals Impacts of Climate Change An Assessment of Vulnerability*.

Jones, P.D., New, M., Parker, D.E., Martin, S., and Rigor, I.G. 1999. Surface air temperature and its changes over the past 150 years. *Reviews of Geophysics* 37: Pp 173 – 199.

Knutson, T.R., and Manabe, S. 1998. Model assessment of decadal variability and trends in the tropical Pacific Ocean. *Journal of Climate*, Sept.

Kay, R., Kirkland, A. and Stewart, I. (1996). Planning for future climate change and sea-level rise induced coastal change in Australia and New Zealand. In *Greenhouse: coping with Climate Change,* Bouma, W.J., Pearman, G.I. and Manning, M.R. (eds). CSIRO Publishing, Melbourne, pp. 377 – 398.

Levitus, S., Antonov, J.I., Boyer, T.P., and Stephens, C. 2000. Warming of the world ocean. *Science*. 287: Pp 2225 – 2229.

Mann, M.E., Bradley, R.S., and Hughes, M.K. 1998. Global-scale temperature patterns and climate forcing over the past six centuries. *Nature* 392: Pp 779 – 787.

Mitchell, N.D. and Williams, J.E. 1996: The consequences for native biota of anthropogenic-induced climate change. In: *Greenhouse; Coping with Climate Change,* Bouma, W.J., Pearman, G.I., and Manning, M.R. (eds)]. CSIRO Publishing, Melbourne, Australia, pp. 308 – 324.

Moore, E.J. and Smith, J.W. 1996. Migration in Response to Climate Change. In *Greenhouse:Coping with Climate Change,* Bouma, W.J., Pearman, G.I., and Manning, M.R. (eds), CSIRO Publishing, Melbourne, pp. 325 – 345.

McKeon, G.M., Howden, S.M., Silburn, D.M., Carter, J.O., Clewett, J.F., Hammer, G.L., Johnson, W., Lloyd, P.L., Mott, J.J., Walker, B., Weston, E.J. and Wilcocks, J.R. (1988). The effect of climate change on crop and pastoral production in Queensland. In *Greenhouse; Planning for Climate Change,* Pearman, G.I.(ed.), CSIRO, Melbourne, pp. 546 – 563.

Morton, S.R., Stafford Smith, D.M., Friedel, M.H., Griffin, G.F., and Pickup, G. 1995: The Stewardship of arid Australia: ecology and landscape management. *Journal of Environmental Management*, 43, 195 – 217.

O'Neill Graeme 1999: Cyclone warnings. Ecos Apr-Jun99 Issue 99, p20.

Paté-Cornell, E. 1996. Uncertainty in global climate change estimates. *Climate Change* 33: Pp 145 – 149.

Peters, R.L., 1992: Conservation of biological diversity in the face of climate change. In: *Global Warming and Biological Diversity*, Peters, R.L. and Lovejoy, T.E. (eds). Yale University Press, New Haven, CT, USA and London, United Kingdom, pp 15 – 26.

Retallack S. and Bunyard P. 1999. We're Changing our Climate Who Can Doubt It?. *The Ecologist* Vol 29 number 2.

Smith and Dukowicz 1993. Climate, the Ocean, and Paralle. Computing. *Los Alamos Science* Number 21.

Steffen and Tyson. 2003. Global change and the earth system: a planet under pressure. In *Climate Change. A Reader.* UNISA. UNISA Press. Pp 265 – 280.

Salinger, M.J., Allan, R., Bindoff, N., Hannah, J., Lavery, B., Lin, Z., Lindesay, J., Nicholls, N., Plummer, N., and Torok, S. (1996). Observed variability and change in climate and sea-level in Australia, New Zealand and the South Pacific. In *Greenhouse: Coping with Climate change,* Bouma, W.J., Pearman, G.I., and Manning, M.R., (eds), CSIRO Publishing, Melbourne, pp. 100 – 126.

Schimmelpfennig, D. Lewandrowski, J. Reilly, J. Tsigas, M. and Parry, I. 1996: Agricultural Adaptation to Climate Change Issues of Longrun Sustainability. Washington DC: U.S. Dept of Agriculture, Economics Research Services. Agricultural economic Report; No: 740.

Trenberth, K.E 1996. Global climate change. From an Abstract of Remarks by Scientists at the National Press Club, Washington, D.C., *Climate Analysis Section, Newsletter 1* (1).

Turner, K., O'Riordan, T., and Kemp, R. 1991. Climate change and risk management. In *Climate change: science, impacts and policy: proceedings of the Second World Climate Conference.* (eds) Jäger, J., and Ferguson, H.L. Cambridge: Cambridge University Press. Pp 397 – 408.

Van Rood 2000. The Heat is On – Climate Change in The New Millenium. *Habitat Australia*: v28 i4 p28.

Van Rood 2000: The Heat is On - - Climate Change in the New Millenmium. *Habitat Australia v28 i4 p28*.

Vellinga, P. and van Verseveld, W.J. 2000. Climate Change and Extreme Weather Events. WWF. Sept.

Viner and Agnew .1999. Climate change and Its impacts on Tourism. Report prepared for WWF-UK: Climate Research Unit, University of East Anglia, Norwich, UK.

Weston, E.J., Harbison, J., Leslie, J.K., Rosenthal, K.M. and Mayer, R.J. (1981). Assessment of the agricultural and pastoral potential of Queensland. *Agriculture Branch Technical Report No 27.* Queensland Department of Primary Industries, Brisbane.

WWF Climate Change Campaign. [a] 1999: Global Warming: The Oceans in Peril.

WWF. [b] 1999: Global warming & Atlantic Hurricanes Backgrounder from WWF International, September.

International Journal of Ecology & Development (IJED),
Winter 2006, Vol. 4, No. W06; Int. J. Ecol. Dev.; 23-34
ISSN 0972-9984; Copyright © 2006 IJED, ISDER

Measuring Socioeconomic Influences On Land Use Distribution at Watershed Level: A Multinomial Logit Analysis

Gandhi Raj Bhattarai[1*], **Daowei Zhang**[2] and **Upton Hatch**[3]

[1]Agricultural Economics and Rural Sociology
Auburn University, Auburn, AL 36849
e-mail: bhattgr@auburn.edu

[2]School of Forestry and Wildlife Sciences
Auburn University, Auburn, AL 36849
e-mail: zhangd@auburn.edu

[3]Auburn University Environmental Institute
Auburn University, Auburn, AL 36849
e-mail: hatchlu@auburn.edu

ABSTRACT

Allocation of fixed proportions of land to developed, agricultural, forest, and other uses in a watershed was modeled as an optimization problem faced by a single user. Two time period cross-sectional data for 60 watersheds were used in the analysis. A multinomial logit model was used to explain the effect of population density, mean age, market concentration, travel time to work, road accessibility, personal income, education level and longitude and latitude of watersheds. Developed land use share was positively related to higher market concentrations and road accessibility, but with a higher average time to work, suggesting a rural-urban job interface. Personal income had significant and negative influence in agricultural land share, which in contrast, was increased with higher proportion of people with college degrees. As the largest city in the study area is blocked by a major river in its west, longitude had a negative influence on developed land share and a positive influence on agricultural, forest and other land use. Latitude positively influenced developed, agricultural and other land shares but negatively influenced share of forestland as the study area is on U.S. costal plains.

Keywords: multinomial logit, land use, watershed

INTRODUCTION

Increasing population and economic activities demand more land for development purposes, such as home sites, roads, airports, schools, parks, and industrial and commercial developments. Population growth and increased per capita disposable income have been important components of the economic demand for urban land uses (Reynolds, 2001). As a result, more land has been cleared of forest for

* Corresponding Author

cultivation and more agricultural lands have been used to satisfy increasing demand for urban development. Urban areas have become more intensified, and they have expanded into rural areas to accommodate the demand for urban land uses. This has created strong competition between urban expansion and agriculture, forestry and other rural land use (Reynolds, 2000).

The southeast region of the United States has experienced tremendous urban expansion and market influence in the past forty years. Georgia ranked 6th among the fastest growing states with a 26.4% increase in population between census years 1990 and 2000. Columbus is among the rapidly growing urban areas in Georgia. While the population of Columbus increased just 4.0% between census years 1990 and 2000, the population in neighboring Harris County increased by a record 33.2% (Census 2000). Some areas within the state have gone through rapid transformation from rural to developed land in a short period of time. However, some parts of the states are still predominantly rural with low population growth and no urban development. While large urban areas have expanded significantly to the suburban areas, more importantly, small townships have developed into urban centers. These discontinuous development and land use change are often regarded as urban sprawl (Carrion-Flores and Irwin, 2004; Wu and Plantinga, 2003).

Individual landowners' decision of land use conversion aggregate into a pattern in regional land use distribution. The level of economic activities, demographic changes, and public policies related to land management are associated with the distribution of agricultural, forest, urban, and other lands. The conversion of land use from forest or agricultural to residential development tends to be permanent and irreversible (Hite, Soghen and Templeton, 2003).

Increased land use in agriculture results in larger quantities of chemicals and pesticides causing higher non-point source pollution of ground and surface water. Clear cutting forests results in loss of wildlife habitat and increases runoff as protective vegetative cover of the soil is lost. Urban development increases the amount of impervious surface and causes higher run-off. Urban wastes such as in landfill sites also cause water pollution when water flows through the wastes.

A combination of all these factors contributes to water stress, pollution, and loss of aquatic and terrestrial biodiversity. Ecosystem services in a watershed are affected by human impact on land and water. Understanding the causes and effects of land use change helps in making public policy towards land development and planning.

The present study develops an econometric model to explain the changes in land use distribution as a function of different levels of demographic, economic and market conditions at the watershed level using time-series cross-sectional data. Impacts on land use distribution for changes in socioeconomic variables are simulated and overall land use scenarios are predicted.

LITERATURE REVIEW AND ANALYTICAL FRAMEWORK

Most land use studies have lately focused on urban sprawl and its effect on agricultural land values, farmland retention and some relationship between the rural-urban interfaces (e.g., Baumol and Oates, 1998; Bearlieu et al., 1998; Onal et al, 1997; Phinn and Stanford, 2001; Reynolds, 2001; Wear and Bolstad, 1998; Hsieh,

Irwin and Forster, 2000; Miller and Plantinga, 1999). Mostly these studies have used aggregate cross-sectional data at county-level for analysis. Few studies, however, have recently tried to explain the land use conversion at micro level (e.g., Hite, Sohngen and Templeton, 2003; Carrion-Flores and Irwin, 2004; Hua, Hite and Sohngen, 2005). Recent studies have used complex models like survival analysis (Hite, Sohngen and Templeton, 2003) and Markov-Chain techniques (Hua, Hite and Sohngen, 2005) to determine both the reasons and timing of land use conversion. Few other studies have given focus to the location and timing of development (Carrion-Flores and Irwin, 2004; Irwin and Bockstael, 2002). However mainstream studies exploring the causes of land use conversion widely used probability based models including multinomial logit or probit models (McMillen, 1989; Buldoc, Fortin and Gordon, 1997; Hardie and Parks, 1997; Plantinga, Mauldin and Miller, 1999; Nagubadi and Zhang, 2005).

These previous studies using multinomial logit models of land use change have mostly focused on the effect of urbanization in the agricultural land values, agricultural and forest interaction, urban-rural interface and land use competition, using land use change as a function of particular regulation, economic activity and population growth at micro level. However, the nature of land use conversion over a wider geographic coverage with respect to population changes, economic growth, and market pressure is not fully explained.

Population growth, urban development, and personal income from non-farm sources are expected to encourage conversion of low return forest and agricultural land to high return developmental use. Increased demand for developmental land causes sharp increase in the price of land in city centers, which gradually expand to the surrounding areas in search of relatively cheaper land, thus reducing the effect of urban expansion with gradual increase of distance from major populated places and city centers. A larger proportion of people employed in non-farm activities within the place of residence suggest a market concentration in the area. However, a higher commute time for regular work, on the other hand, indicates possible urban traffic congestion. Similarly, population structure such as average age of the people in an area also affects the demand for lands for alternative uses. People's expectation about the returns from alternative uses of land affects their decision to allocate available lands in different uses.

In this study, the allocation of fixed proportion of lands to different developed, agricultural, forest and other uses in a watershed was viewed as an optimization problem faced by a single user. To avoid structural complexity of externalities, the model has been kept to the simplest form without introducing externalities. Land use is taken as a function of population density, average age, personal income, education level, employment concentration, commute time, accessibility and spatial location.

The variables such employment concentration, commute time and road accessibility were taken as indicators of urban development and market concentration. Employment concentration is measured by a ratio of people involved in non-farm employment within place of residence and accessibility is measured by the amount of transportation network and commercial infrastructure in the area. Similarly, population density, average age and education level were taken as an indicator of demographic structure. Population density is measured in terms of persons per square miles of surface area. Average age is mean of all people's age in each

watershed. Personal income is taken as an indicator of economic development in the area, which is expressed in thousand dollars. Education level is expressed as the ratio of people having at least bachelors level education to the total population.

Relative spatial location is expressed in terms of longitude and latitude of the centroid of watershed. If latitude and longitude have significant marginal effects on land use choice, it will suggest a spatial pattern in the land use distribution in the area.

A modified multinomial logit model from Parks (1980) is used for the analysis. Land use in each category is expressed as the share of total area of land in each type in the watershed, the sum of which equals one. Since the land is fixed in a given watershed, increase in the share of one type of land results in equal decrease in other land use shares. Thus if we know the current shares (proportions) of different land uses in a given watershed, we can estimate the changes and determine new shares by the probability each land use type is impacted by changes in the explanatory variable. A system of simultaneous equations, one equation for each type of land use, can solve this problem by jointly determining the model.

Thus we try to derive the proportion of each type of land in a given watershed by solving a probability-based model as given below.

$$P_{ikt} = \frac{\exp(\beta'_k X_{it})}{\sum_{k=1}^{K} \exp(\beta'_k X_{it})} \qquad (1)$$

where, *p* is the proportion of land in i^{th} watershed, in k^{th} use and at time *t*. **X** represents a vector of demographic, economic and spatial characteristics for the observed individual watershed. β_{it} is a vector of estimated parameters.

Normalization of equation (1) by one of the land use shares (for example, k=4 and constraining β_4=0) yields the multinomial logit model as:

$$P_{ikt} = \frac{\exp(\beta'_k X_{it})}{1 + \sum_{k=1}^{K-1} \exp(\beta'_k X_{it})} \qquad \text{for k=1, 2, … K-1} \qquad (2)$$

The proportion of omitted (4^{th}) category is derived from the formula:

$$P_{i4t} = \frac{1}{1 + \sum_{k=1}^{K-1} \exp(\beta'_k X_{it})} \qquad (3)$$

In order to simply the models, equation (1) is transformed logarithmically to yield the following three (K-1) equations:

$$\ln(P_{ikt} / P_{i4t}) = \beta_k X_{it} + u_{it} \qquad \text{for k = 1, …, K-1} \qquad (4)$$

where u_{it} is the random error terms. However, the optimal land use proportions or P_{ikt} in the above equations are not directly observable, we replace these values with the observed actual land use proportions for the model estimation. Thus the model to be estimated is a system of three equations which are linear in parameters.

$$\ln(y_{ikt} / y_{i4t}) = \beta_k X_{it} + u_{it} + \varepsilon_{ikt} \text{ for k = 1, …, K-1} \quad (4)$$

Since the coefficients of such models are not directly interpretable in terms of marginal effects as in OLS, marginal effects were estimated to express the probability of change in land use with respect to each independent variable measured from the mean of the variable:

$$\frac{\partial y_{ikt}}{\partial x_{ikt}} = \left(\beta_{kx} - \sum_{k=1}^{K-1} y_{ikt}.\beta_{kx} \right).y_{ikt} \text{ for k=1, …, K-1} \quad (5)$$

where, β_{kx} is the coefficient of x for land use k. The marginal effect on the redundant category is obvious as the sum of the marginal effects of all categories equals to zero.

DATA AND METHODS

Five western Georgia counties, Harris, Meriwether, Muscogee, Talbot and Troup were selected to represent different transitions of land use change in the study area. The analysis was done at the 12-digit hydrological unit watershed level taken from Georgia Spatial Data Clearing House. A total of 60 watersheds were selected within the five-county boundaries, which ranged in size from 2,693 acres to 30,643 acres with a mean of 16,556 acres. A few of the larger watersheds were divided into smaller sub-watersheds using geographic information system tools.

The National Land Cover Database (NLCD) was obtained for calendar year 1990 and 1998. The first 21-class digital land cover map (NLCD 1992) was obtained from the United States Geological Survey which was based on the satellite images circa 1988-1990. The second set of 18-class land cover map was obtained from the Georgia Spatial Data Clearing House which was developed based on the satellite images taken during 1996-1998. Digital land use maps were converted to grids and reclassified into four broad land use categories namely “developed”, “agricultural”, “forest” and “other”.

Census Block Group (CBG) level housing and population data (STF3A Microdata) were obtained from the Interuniversity Consortium for Political and Social Research database (ICPSR). This data set contained information on population structure such as total counts and percentages in rural versus urban areas, age structure, personal and household income, education, family structure, characteristics and counts of housing units, median house value among others. All monetary values were deflated to base year 100 for 1984.

Topologically Integrated Geographic Encoding and Referencing System (TIGER) line data for census block groups were obtained from the US Census Bureau. Tabular form socioeconomic data were spatially joined with the TIGER line table. Assuming a uniform distribution of information within each census block group, the census block level data was spatially transferred to watershed level using the ‘two-theme’ tool in ArcView GIS. Data analysis was done using SAS program.

RESULTS AND DISCUSSIONS

Descriptive statistics of the study variables are given in Table 1. The population density and the average age of population both increased by 5% between the two census periods. In general, the number of people working at the place of residence decreased by 9% while travel time to work increased by 18%. This pattern provided evidence of urban traffic congestion and rural urban job interface. The transportation network, defined as the total land surface under roads and railway network, increased by 323%. Per capita income increased by 23% and proportion of population with bachelors and higher degree increased by 31%. In general, the weighted share of land use in developmental use increased by 187% while agricultural and forestland decreased by 19% and 6% respectively.

The model was estimated as a system of three equations. The equations for developed, agricultural and forestland shares were jointly determined using iterated seemingly unrelated regression (ITSUR). Both the Bruesch-Pagan and White's test showed presence of heteroskedasticity on population density and local job ratio variables in the developed land equation. An attempt to correct heteroskedasticity by weighting the local job ratio and population density further worsened the error structure. Correcting for heterosckedasticity by weighting for average age resulted in non-significant test statistics at the 5% level of significance.

The results of the heteroskedasticity corrected regression models are given in Table 2. The parameter coefficients for such models are difficult to interpret directly. Instead the marginal effects are the only means to effectively interpret the effect of explanatory variables on the distribution of proportion of dependent variables. Marginal effects are the percentage change in the dependent variable with respect to a unit change in explanatory variable, generally measured from the mean. A positive or negative sign of marginal effects, the only reliable indicator in such models, indicates an increase or decrease in the proportion of land in that use. Since the sums of proportions of land in all land use classes should equal one, the marginal effects of explanatory variables on the redundant category can be easily calculated by subtracting the other values from one. Table 2 includes the results for estimation, marginal effects and elasticity of each of the variables in each of the jointly determined models.

Though the marginal effect of population density in developed land was negative but non-significant, the effects were positive and statistically significant for both agricultural and forestland shares. It is assumed that conversion of cotton land to forestland and streamside management practices in recent years contributed to the increase in forestland's share. The increase in forest and agricultural land shares were compensated by reduction in other land uses such as wetland, water bodies and barren lands.

Higher education level, as measured by the ratio of population holding at least a bachelors degree, had positive influence on agricultural land share while negatively affecting forestland, developed land and other land shares. On the other hand, per capita income was not significant in determining the share of developed and forestland while it significantly decreased the share of agricultural land.

Average commuting time had significant effects on all land use shares. Developed land share was positively related to the average commuting time, while agricultural and forestland shares were inversely related to the commuting time. Availability of

jobs in the place of residence, as measured by the ratio of people employed in the place of residence, was significant for developed land share (positive) and forestland share (negative). Market concentration and job availability in the area was associated with more land conversion from forest to developmental uses. Though not significant in any equations, the ratio of commercial/ industrial/ transportation land to the total land positively affected the share of developed land and agricultural land shares while decreased the forest and other land shares.

The longitude coefficient was significant and negatively influenced the share of developed land while positively influenced the agricultural and forestland shares. Everything else being equal, the proportion of developed land would decrease and that of agricultural and forestland share would increase when moving from west (near the center of Columbus metropolitan area) to the east. This suggests a one directional spatial relationship between the distance and urban development. Latitude values were not significant for any equations but had a positive marginal effect on developed, agricultural and other land, and a negative effect on forest and other land. This is because the study area is on the southeastern U.S. costal plains. In short, the proportion of forestland use would decrease towards the north and increase towards the east direction and that the share of agricultural land would increase when moving towards north and to the east. These spatial effects were confirmed by comparing the two land use maps (not shown in this paper).

The models validation was done by forecasting predicted land use shares in both years and comparing them with the observed data. The model correctly estimated the change in land use share for agricultural land and other land. The predictive power of the model was slightly improved by correcting for heteroskedasticity. A simulated land use distribution for current rate of changes on included variables is given in Figure 1. Interestingly, the share of developed land is expected to increase exponentially beyond 2000 at the expense of forestland.

CONCLUSION

This study developed an econometric model to explain land use distribution at the watershed level in five West Georgia counties. A multinomial logit model explains the effect of population density, mean age, employment concentration, commuting time, accessibility, personal income, education level, and longitude and latitude of watersheds. Developed land use share is positively related to higher market concentration and road accessibility. A significant and positive effect of higher commute time on developed land use suggests a rural-urban job interface. Personal income has a negative influence only on the agricultural land share, which in contrast increases with a higher education. Longitude has a negative influence in developed land share and a positive influence on agricultural, forest, and other land use. Latitude has a positive influence on developed, agricultural, and other land shares while negatively influencing the forestland share. These results suggest a spatial pattern of land use distribution in the study area.

ACKNOWLEDGEMENTS

This study was funded by the Center for Forest Sustainability at School of Forestry and Wildlife Sciences, Auburn University, Alabama, USA. Appreciation is expressed to Diane Hite and Henry Thompson for review and helpful comments.

REFERENCES

Baumol, W.J. and Oates, W.E., 1998, *The Theory of Environmental Policy*, 2nd Ed. Cambridge University Press.

Bearlieu, J., Bennett, D., Kraft, S. and Sengupta, R., 1998, *Ecological-Economic Modeling on a Watershed Basis: a case study of the cache river of Southern Illinois.* Paper presented at the AAEA Annual meeting, Salt Lake City, Utah, 1998.

Buldoc, D., B Fortin and S. Gordon, 1997, *Multinomial Probit Estimation of Spatially Independent Choices: An Empirical Comparison of Two New Techniques.* International Regional Science Review, 20, 77-101.

Carrion-Flores, C. and Irwin, E., 2004, *Determinants of Residential Land-Use Conversion and Sprawl at the Rural-Urban Fringe*. American Journal of Agricultural Economics, 86, 4, 889-904.

Hardie, I.W., and Parks, P.J., 1997, *Land Use with Heterogeneous Land Quality: An Application of an Area Base Model.* American Journal of Agricultural Economics, 79, 2, 299-310.

Hite, D., Sohngen, B. L., and Templeton, J., 2003. *Zoning, Development Timing, and Agricultural Land Use at the Suburban Fringe: A Competing Risks Approach.* Agricultural and Resource Economics Review, 32, 1, 145-157.

Hsieh, W., Irwin, E.G., and Forster, L., 2000, *Spatial Dependence among County-Level Land Use Change.* Paper presented at the American Agricultural Economics Association Annual Meeting, Tampa, Florida, U.S., August 2000.

Hua, W., Hite, D., and Sohngen, B., 2005. *Assessing the Relationship Between Crop Choice and Land Use Using a Markov Model.* Paper presented at the American Agricultural Economics Association Annual Meeting, Providence, RI, USA, July 24-27, 2005.

Irwin, E.G., and Bockstael, N.E., 2002, *Interacting Agents, Spatial Externalities and the Evolution of Residential Land Use Patterns.* Journal of Economic Geography, 2, 1, 31-54.

McMillen, D.P., 1989, *An Impirical Model of Urban Fringe Land Use.* Land Economics, 65, 2, 138-145.

Miller D.J., and Plantinga, A.J., 1999, *Modeling Land Use Decisions with Aggregate Data.* American Journal of Agricultural Economics, 81, 1, 180-194

Nagubadi, R.V., and Zhang, D., 2005, *Determinants of Timberland Use by Ownership and Forest Type in Alabama and Georgia.* Journal of Agricultural and Applied Economics, 37, 1, 173-186.

Onal, H., Algozin, K.A., Isik, M., 1997, *Environment, Equity and Watershed Management.* Paper presented at the American Agricultural Economics Association, Toronto, Canada; July 1997.

Parks, R.W., 1980, *On the Estimation of Multinomial Logit Models from Relative Frequency Data*. Journal of Economics, 13, 293–303.

Phinn, S. and Stanford, M., 2001, *Monitoring Land-Cover and Land-Use Change in a Rapidly Urbanizing Coastal Environment: the Maroochy and Mooloolah Rivers catchments, Southeast Queensland, 1988-1997*. Australian Geographical Studies, 39, 2, 217-232.

Plantinga, A.J., Mauldin, T, and Miller, D.J., 1999. An Econometric Analysis of the Costs of Sequestering Carbon in Forests. American Journal of Agricultural Economics, 81, 4, 812-824.

Reynolds, J.E., 2000, Florida Rural Land: C*ompetition Between Agricultural and Urban Uses*. Soil and Crop Science Society of Florida Proceedings 59, 94-98.

Reynolds, J.E., 2001, *Land Use Change and Competition in the South*. Journal of Agricultural and Applied Economics, 33, 2, 271-281.

Templeton, S.T., 2004, Demographic, Economic and Political Determinant of Land Development in the U.S. U.S. Paper presented at the American Agricultural Economics Association Annual Meeting, Denver, CO, July 1-4, 2004.

U.S. Dept. of Commerce, Bureau of the Census. *Census Of Population And Housing, 1990 [United States]: Summary Tape File 3A* [Computer file]. Washington, DC: U.S. Dept. of Commerce, Bureau of the Census [producer], 1993. Ann Arbor, MI: Inter-university Consortium for Political and Social Research [distributor], 1999

U.S. Dept. of Commerce, Bureau of the Census. *Census Of Population And Housing, 2000 [United States]: Summary File 3, Georgia* [Computer file]. Washington, DC: U.S. Dept. of Commerce, Bureau of the Census [producer], 2002. Ann Arbor, MI: Inter-university Consortium for Political and Social Research [distributor], 2002.

United States Census Bureau, 2000 (Census 2000), *State and County Quick Facts*. http://quickfacts.census.gov/qfd/index.html

United States Geological Survey, National Center for Earth Research Observation and Science (EROS). http://seamless.usgs.gov

Wear, D.W., and Bolstad, P., 1998, *Land-Use Change in the Southern Apalachian Landscpaes: Spatial Analysis and Forecast Evaluation.* Ecosystems, 1, 575-594.

Wu, J., and Plantinga, A., 2003. *The Influence of Public Open Space on Urban Spatial Structure.* Journal of Environmental Economics and Management, 46, 288-309.

Table 1. Descriptive statistics of variables used in the study

Variables	1990		2000		Change
	Mean	**Std.**	**Mean**	**Std.**	**%**
Population density	0.121	0.118	0.127	0.113	5%
Average age	35.027	2.544	36.868	2.437	5%
Local job ratio	0.275	0.317	0.251	0.317	-9%
Travel time to work in minutes	23.112	4.584	27.196	6.527	18%
Transportation network (land surface area)	0.020	0.042	0.084	0.080	323%
Personal income ($ '000)	8.790	2.824	10.853	3.279	23%
Education level	0.148	0.078	0.193	0.095	31%
Longitude	-84.823	0.167	-84.823	0.167	0%
Latitude	32.786	0.203	32.786	0.203	0%
Land use distribution (ratio)					
Developed	0.077	0.182	0.145	0.191	187%
Agricultural	0.104	0.063	0.084	0.060	-19%
Forestry	0.773	0.172	0.723	0.176	-6%
Other	0.045	0.034	0.047	0.040	5%

Table 2. Results of multinomial logit model

	Developed			Agricultural			Forestland		
Variables	Coeff.		M.E.	Coeff.		M.E.	Coeff.		M.E.
Intercept	-239.76	**		-7.421			10.425		
	(114.5)			(63.679)			(50.483)		
Population density	1.295		-0.015	2.432	*	0.062	1.747	*	0.023
	(2.235)			(1.242)			(0.985)		
Average age	0.161	**	0.004	0.055		0.001	0.041		-0.003
	(0.076)			(0.042)			(0.033)		
Work in place	2.98	**	0.139	-0.825		0.019	-1.285	**	-0.201
	(1.192)			(0.662)			(0.525		
Travel time to work	0.114	**	0.005	-0.057	**	-0.002	-0.044	**	-0.005
	(0.045)			(0.025)			(0.02)		
Road Network	5.357		0.213	-0.506		0.027	-1.145		-0.273
	(3.516)			(1.955)			(1.55)		
Per capita income	-0.006		0.003	-0.198	***	-0.009	-0.09		0.002
	(0.124)			(0.069)			(0.055)		
Education level	2.407		-0.037	5.727	**	0.196	3.458	*	-0.017
	(4.54)			(2.524)			(2.00)		
X-Coordinate	-2.354	*	-0.071	0.085		0.032	-0.249		0.028
	(1.382)			(0.768)			(0.609)		
Y-Coordinate	0.906		0.054	0.481		0.099	-0.867		-0.179
	(1.11)			(0.617)			(0.489)		
Adjusted R^2	0.30			0.12			0.08		
Obs.	120			120			120		

***Significant at 1% level, **Significant at 5% level; *Significant at 10% level

M.E. = Marginal Effects; Coeff. = Parameter Coefficients

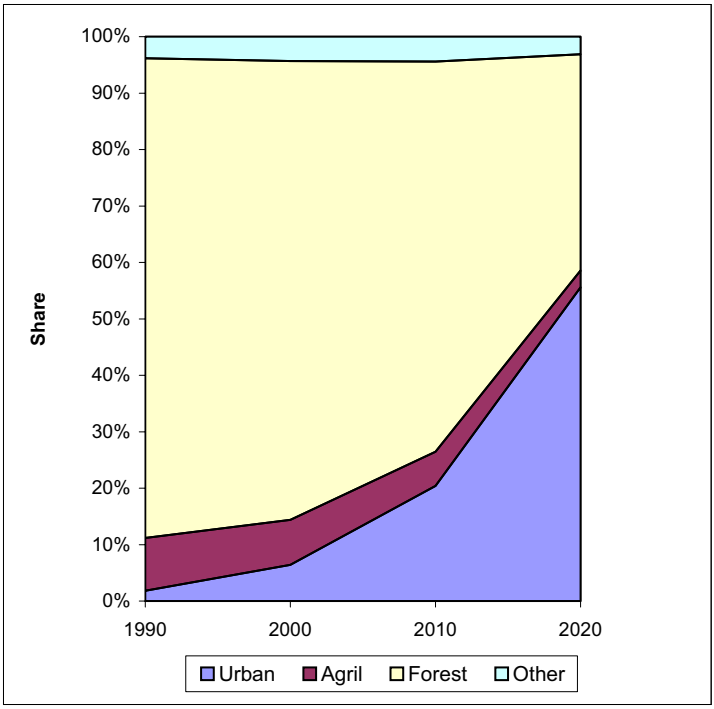

Figure 1. Prediction of land use at current growth rate

International Journal of Ecology & Development (IJED),
Winter 2006, Vol. 4, No. W06; Int. J. Ecol. Dev.; 35-51
ISSN 0972-9984; Copyright © 2006 IJED, ISDER

Effect of Inclusion of a Synthetic Vortex on the Prediction of a Tropical Cyclone over the Bay of Bengal Using a Mesoscale Model

S. Sandeep [1], A.Chandrasekar [1*] and S.K.Dash [2]

[1] Department of Physics & Meteorology,
Indian Institute of Technology Kharagpur, India

[2] Centre for Atmospheric Sciences,
Indian Institute of Technology, New Delhi, India
* E mail: chand@phy.iitkgp.ernet.in

ABSTRACT

Tropical cyclones form over the data-sparse sea regions and hence are analyzed very poorly. This results in initial errors, which may impact on the cyclone track forecast. A solution to the above is to remove the weak initial vortex and replace it with a synthetic vortex (with the correct size, intensity and location) in the initial analysis. The objective of this study is to investigate the impact of introducing a synthetic vortex (based on the NCAR-AFWA scheme) using the regional model MM5 on a tropical cyclone, which formed over the Bay of Bengal during November 2002. It is found that inclusion of the synthetic vortex has caused improvement in the simulation of wind asymmetries and warm temperature anomalies. The central minimum pressure and the maximum wind speed of the simulations with synthetic vortex are lower by 12 hPa and higher by 12 m sec $^{-1}$ as compared to the simulations without the synthetic vortex. Also, this has resulted in a considerable reduction of the track prediction errors: 168 km in 06 hours, 109 km in 12 hours, 332 km in 18 hours, 601 km in 24 hours and 126 km in 30 hours of forecast. However, the impact of synthetic vortex reduces after 30 hours and the track error is higher by 80 km in 36 hours and 284 km in 42 hours of forecast.

KEYWORDS

Synthetic vortex, MM5, NCAR, AFWA, tropical cyclone, Bay of Bengal

1.1 INTRODUCTION

Since tropical cyclones form over the data sparse sea regions they are often analyzed very poorly, with centers ill defined and in the wrong location. Most of the tropical cyclone models/mesoscale models utilize three-dimensional analysis as initial conditions, which are themselves, model outputs from global coarse resolution models. A tropical cyclone in such an analysis is invariably weaker and more diffuse. The above may seriously impact on the model performance of the forecast of

the cyclone's track and intensity changes. A solution to the above is to remove the weak vortex in the initial cyclonic structure and replace it with a synthetic vortex, which is closer to the observations as far as the size, intensity and location are concerned. Three approaches exist in the literature for the initialization of tropical cyclone: (1) substitute a specified vortex circulation, defined mostly by an analytical expression, for the analyzed vortex into the initial conditions (Mathur [1991] and Leslie and Holland [1995]), (2) implant a "spinup" vortex generated by the same forecast model into the initial conditions (Kurihara et al. [1993]), and (3) improve the initial conditions by making use of satellite–raingauge based measurements of rainfall through a physical initialization procedure (Krishnamurti et al. [1993]). Davis and Low-Nam [2001] have recently proposed the National Center for Atmospheric Research (NCAR) - Air Force Weather Agency (AFWA) tropical cyclone synthetic vortex scheme that is now provided as a part of the NCAR- Pennsylvania State University (PSU) Fifth Generation Mesoscale Model (MM5) (Grell et al. [1994]).

Roy Abraham et al. [1995] studied the impact of inclusion of two synthetic vortices (Rankine vortex and Holland vortex) to simulate two tropical cyclones, which had formed over India during May 1979 and August 1979. The results of the above study indicated that the simulations with Rankine vortex indicated tracks to the left of the observed while the simulations with Holland vortex showed tracks to the right of the observed tracks. The results of the simulation with Holland vortex indicated that the system moved faster compared to the simulations with the Rankine vortex. Prasad [2005] performed numerical experiments with a quasi-Lagrangian limited area model for several cyclones which have formed over India. Trivedi et al. [2002] have recently investigated the impact of the initial conditions on the numerical simulation of a super cyclonic storm over Bay of Bengal, India, which crossed the Orissa coast on 29 October 1999 using the MM5 model. They generated the synthetic vortex data using the same scheme as Mathur [1991]. They also performed four-dimensional data assimilation to assimilate the synthetic vortex in the initial stage to the model. The results of the above study indicated considerable improvement in the track of the super cyclone due to the inclusion of the synthetic vortex. Their study successfully simulated the typical features of a tropical cyclone, such as asymmetries in the wind field with the strongest winds occurring to the east and close to the cyclone's center. Also, the results indicated that strong wind gradients were found between the center and the maximum wind region and there was a slow decrease in wind speed up to

the middle troposphere. However, the above inclusion of the synthetic vortex could not predict the observed/estimated 98 hPa pressure drop in the central sea level pressure field associated with the Orissa super cyclone (Trivedi et al. [2002]). Mohanty et al. [2004] utilized the MM5 model to simulate the above-mentioned super cyclone using NCEP reanalysis. To get the necessary small-scale features, Mohanty et al. [2004] integrated the MM5 model for 12 hours with analysis nudging before the start of the actual forecast. The resultant simulated track showed reasonable agreement with the observed track with a vector displacement error of 196 km, 157 km, 197 km, 137 km and 302 km at the end of 24 hours, 48 hours, 72 hours, 96 hours and 120 hours, respectively. The MM5 model was utilized to study the 1998 Hurricane Earl which hit Florida, United States and the 1999 Orissa Supper cyclone by Rao and Bhaskara Rao [2003].

The chief objective of this work is to investigate the impact of inclusion of the NCAR-AFWA synthetic Rankine vortex on the track forecast of a tropical cyclone, which formed over the Bay of Bengal during November 2002 using the MM5 model. The NCAR-AFWA synthetic vortex scheme is likely to remove the weak and diffuse cyclonic vortex in the initial analysis and replace it with an axi-symmetric Rankine vortex with the correct size, strength (as estimated from the maximum winds) and location as obtained from observations. The major problem in such schemes is that the poorly analyzed diffuse weak vortex in the first guess (analysis) must be removed completely. If the above is not done properly, the ghost vortex can cause severe degradation of the cyclone track forecast. Also, it is to be noted that the available observations in the tropical cyclone vicinity has to be used in an optimum manner. Another major problem is that the addition of the synthetic vortex can introduce significant shocks to the system in the early model integration, which can even degrade the subsequent model forecast. Kurihara et al. [1993] has suggested an approach, which utilizes an initial smoothing of the fields in the tropical cyclone vicinity followed by insertion of the synthetic vortex using a non-linear balance equation to tackle the ghost vortex problem. Also, using a very well balanced vortex would considerably reduce the model shock due to insertion of the synthetic vortex (Kurihara et al. [1993]). Since the NCAR-AFWA ensures nonlinear balance of mass and wind fields and uses a nicely balanced vortex it would appear that both the ghost vortex problem and the model shock problem can be handled effectively. It is expected that the removal of the weak and diffuse cyclonic vortex in the analysis and

inclusion of a synthetic Rankine vortex in the analysis would improve the initial size, initial strength (in terms of radius of maximum wind and the vortex wind at the radius of maximum wind) and the initial location of the tropical cyclone. With an improved initial cyclonic structure and a model, which has all the important physical processes, which occur in the real nature, it is expected that the model will simulate the well-known characteristic features of a tropical cyclone and will lead to an overall improvement in the model performance especially in its track prediction.

1.2 NCAR-AFWA synthetic vortex scheme

The NCAR-AFWA tropical cyclone synthetic vortex scheme can be envisaged as primarily made up of two components (Davis and Low-Nam [2001]). The first component provides for detection and extraction of tropical cyclone from the analysis (first-guess field) while the second component deals with the calculation of the synthetic vortex and blending of the same together with a modified background field to form the final analysis. The first step in the removal of the weak vortex is to identify the center of the vortex. This is accomplished by searching for the maximum vorticity on the analysis pressure level nearest to the surface within a prescribed radial distance (400 km) from the Best Track location of the tropical cyclone. Davis and Low-Nam [2001] modified the vorticity, geostrophic vorticity and divergence fields and calculated the change in the non-divergent stream function, geopotential and velocity potential and using the above computed a modified velocity field. The above approach varies from that of Kurihara et al. [1993] where a sophisticated filtering scheme is used to remove the weak initial vortex. The synthetic vortex (Davis and Low-Nam [2001]) which replaces the weak initial vortex in the NCAR-AFWA scheme has the following features (i) axisymmetry, (ii) fixed radius of maximum wind (normally is taken as twice the grid resolution), (iii) nonlinear balance of mass and wind fields, (iv) nearly saturated (with respect to water or ice), (v) no eye and (vi) maximum winds of the synthetic vortex are a pre-determined fraction of the observed maximum winds. The vortex wind profile is considered as a simple vortex of the Rankine type with the tangential wind given by,

$$v = A(z)\, F(r) ;$$

$$F(r) = \frac{v_m}{r_m} r ; \quad (r \le r_m)$$

$$F(r) = \frac{v_m}{r_m^{\alpha}} r^{\alpha} ; (r > r_m)$$

where F(r) is the radial dependence and A(z) is the amplitude and vertical dependence, r_m and v_m are the radius of maximum wind and the maximum wind at r_m and α is a parameter. The vertical weight function A(z) is assigned a value of unity from the surface through 850 hPa, 0.95 at 700 hPa, 0.9 at 500 hPa, 0.7 at 300 hPa, 0.6 at 200 hPa and 0.1 at 100 hPa. More details of the NCAR-AFWA scheme are available in Davis and Low-Nam [2001] and hence are not mentioned here. Section 2 outlines a synoptic description of the tropical cyclone while Section 3 provides a description of the model and design of the numerical experiments. The results and discussions are presented in Section 4 while the conclusions of the study are reported in Section 5.

2. SYNOPTIC FEATURES OF THE TROPICAL CYCLONE

The tropical cyclone, which is being investigated in this study, was first noted as a depression 235 km east-southeast of Chennai, India at 06 UTC on 10 November 2002. The depression moved steadily northeastward and intensified to gale force at 12 UTC on 11 November and was centered 750 km south-southwest of Kolkata, India. The intensity of the system did not change until the 12th November when it accelerated in the northeast direction and was located 195 km south-southwest of Kolkata with a maximum wind speed of 28 m sec $^{-1}$ and a minimum pressure of 988 hPa. The above cyclone crossed Sagar island at 09 UTC on 12 November 2002 and quickly weakened to a depression by 12 UTC. The above system did inflict about 50 casualties and caused damages during its lifetime.

3. MODEL DESCRIPTION AND NUMERICAL EXPERIMENTS

The present study utilized the MM5 version 3.6 (Grell et al. [1994]). The model was configured with twenty three vertical layers (centered at σ = 0.995, 0.985, 0.97, 0.945, 0.91, 0.87, 0.825, 0.775, 0.725, 0.675, 0.625, 0.575, 0.525, 0.475, 0.425, 0.375, 0.325, 0.275, 0.225, 0.175, 0.125, 0.075, 0.025) and two nested domains (Outer Domain: 90 km grid spacing with 85 x 75 grid cells in east-west and north-south directions; Inner Domain: 30 km grid spacing with 130 x 118 grid cells in the east-west and north-south directions). Other model settings included: MRF PBL scheme, the Grell cumulus scheme, a mixed phase Reisner scheme for explicit

moisture, a cloud radiation scheme and a multi-level soil model. The NCEP reanalysis data available at a horizontal resolution of 2.5 ^{o} x 2.5 ^{o} and a time resolution of 6 hours were used to develop the initial and lateral boundary conditions. A one-way nesting option was employed. Two numerical experiments were conceived to study the simultaneous impact of inclusion of the NCAR-AFWA synthetic vortex scheme in the track prediction of a tropical cyclone, which formed in the Bay of Bengal during November 2002. The first experiment (called CTRL) utilized the NCEP reanalysis for the initial and lateral boundary conditions and the model integrations were performed from 10 November 2002 18 UTC to 12 November 2002 12 UTC. The second numerical experiment (called SYN-VOR) included the NCAR-AFWA synthetic vortex scheme and the integrations were performed as in the first experiment. The second experiment used the following values for the parameters α = -0.75, r_m = 90 km, v_m = 25 m s $^{-1}$, vortex size = 300 km and search radius = 400 km. The results of the MM5 simulation corresponding to the two numerical experiments were then compared with NCEP reanalysis as well as with observations for the time period between 10 November 2002 18 UTC to 12 November 2002 12 UTC. The need to investigate the impact of inclusion of the NCAR-AFWA synthetic vortex scheme on the track prediction of a tropical cyclone, which formed over the Bay of Bengal, led us to conceive the second experiment.

4. RESULTS AND DISCUSSIONS

As stated earlier, the objective of this study is to examine the impact of the modified initial conditions brought about through inclusion of a NCAR-AFWA synthetic vortex on the track prediction of a tropical cyclone which formed over the Bay of Bengal during 10 – 12 November 2002. The synthetic vortex being included is considered axi-symmetric partly for convenience and simplicity and mainly due to non-availability of detailed observed asymmetries associated with the tropical cyclone. This is the reason why a pre-determined fraction of the observed maximum wind is utilized in the synthetic axisymmetric vortex so that the remaining may be attributed to the asymmetries. We utilized a model domain, which encompassed the entire India and its immediate neighborhood for the outer 90 km while the inner 30 km domain encompassed most parts of India, the entire Bay of Bengal and the eastern part of Arabian Sea. Since the NCEP reanalysis has relatively coarse resolution, it was found necessary to define a system of two nested domains with horizontal grid spacing of 90 km (D1) and 30 km (D2). All the model results discussed in this study

correspond to the 30 km domain. The model domain is shown in Figure 1a.

Figures 1b-1c depict the time series of the minimum sea level pressure (SLP) and the maximum wind speeds (MWS) from 10 November 2002 18 UTC to 12 November 2002 12 UTC. The above figures provide the NCEP reanalysis, observations as well as the results of the CTRL and SYN_VOR runs. The SLP observations are basically estimated based on the empirical relationship between the MWS and the minimum SLP in tropical cyclones over Bay of Bengal and Arabian Sea using observations from ships, reconnaissance aircraft and the coastal stations (Mishra and Gupta, 1976). Figure 1b shows clearly that the SYN-VOR run has produced a pressure fall in the central pressure from 1003 hPa to 995 hPa in a period of 18 hours and an increase of MWS from about 18 m sec $^{-1}$ to 27 m sec $^{-1}$ in 12 hours. The CTRL run, on the other hand reveal a slight increase of central pressure, a slight fall and a further rise providing a higher pressure of as much as 12 hPa as compared to the SYN-VOR run. Also, the CTRL run, despite showing some rise in wind speed still falls short of the observed wind speed by 7 m sec $^{-1}$. Overall, Figure 1b reveals that while the CTRL run follows the NCEP reanalysis, the SYN-VOR run compares favorably with the observations. Despite the impressive improvement shown in the results (Figure 1b) due to inclusion of synthetic vortex, there is still a 7 hPa pressure fall which is not accounted for by the SYN-VOR run. Also, the SYN-VOR run shows MWS to rise about 12 hours before the MWS rise is seen in the observations (Figure 1c).

Figure 2 depicts the west-east cross-section through the center of the cyclonic storm for the wind speed at the initial, 12, 24 and 36 hours of forecast for both the CTRL and SYN-VOR runs. Trivedi et al. [2002] included a synthetic vortex in the MM5 for the 1999 Orissa super cyclone and successfully simulated the following typical features of a tropical cyclone, such as asymmetries in the wind field with the strongest winds occurring to the east and close to the cyclone's center. Also their results indicate that strong wind gradients were found between the center and the maximum wind region and there was a slow decrease in wind speed up to the middle troposphere. The CTRL run shows some structure at 24 and 36 hours of forecast, however, the slow decrease in wind speed to the middle troposphere to the east of the cyclone center is missing. The SYN-VOR run (Figure 2), however, shows a much more realistic and improved structure with wind asymmetries (stronger wind to the

east of the center and close to the center in the lower troposphere). Also, the SYN-VOR run reveals the existence of strong gradients both inside and outside the region of maximum winds. The gradual decrease in wind speed up to the middle and upper troposphere as simulated by Trivedi et al. [2002] is also reproduced by the SYN-VOR run. All the above-mentioned characteristic features of tropical cyclone simulated with the inclusion of a synthetic vortex are in agreement with the results of Mathur [1991]. Figure 3 depicts the SLP at the initial and for 12, 24 and 36 hours of forecast for both CTRL and SYN-VOR runs. Figure 3 shows that the SYN-VOR run simulates a stronger system (lower SLP and stronger SLP gradients) compared to the CTRL run. The SLP field simulated by the SYN-VOR run is typical of the SLP field associated with a cyclone. Figure 4 depicts the west-east cross-section of the potential temperature (θ) and the vertical velocity through the center of the cyclonic storm at the initial and for 12, 24 and 36 hours of forecast for both CTRL and SYN-VOR runs. The SYN-VOR run has produced a prominent warm core with a warm temperature anomaly in the middle and upper troposphere at 12 hours of forecast (Figure 4) and the warm anomaly gets strengthened at 24 and 36 hours of forecast. The CTRL run, unlike the SYN-VOR run, does not posses a well-marked warm temperature anomaly in the middle and upper troposphere. The SYN-VOR run also simulates strong vertical velocity in and around the regions showing the warm temperature anomaly. The SYN-VOR run shows strengthening of the vertical wind with time with the maximum vertical wind seen at 36 hours of the forecast (12 November 2002 06 UTC). The CTRL run also shows evidence of strengthening of the vertical wind at and after 24 hours of forecast. However, the vertical wind simulated by the CTRL run is weak compared to the SYN-VOR run.

Figure 5 depicts the lower tropospheric winds at the initial, 12, 24 and 36 hours of forecast as well as the 24-hour accumulated precipitation (restricted to 24 hours only) for both the CTRL and SYN-VOR runs. The lower tropospheric winds from the SYN-VOR and CTRL runs refer to $\sigma = 0.995$. The SYN-VOR run simulates a relatively well-defined lower cyclonic circulation with stronger winds as compared to the CTRL run. The SYN-VOR run also simulates a better structure in the spatial distribution of the rainfall at 24 hours as compared to the CTRL run. Figure 6 provides the track prediction of both SYN-VOR and CTRL runs as well as IMD observations and NCEP reanalysis at 6-hour intervals. The observed track shows initial northward movement and then steady northeastward movement. The SYN-

VOR run simulates a track closer to the observations till about 30 hours of forecast. However, the impact of the synthetic vortex reduces on and after 36 hours with the CTRL run showing less track errors for 36 and 42 hours. Table 1 provides for the vector track prediction errors in km with respect to the observations of both the CTRL and the SYN-VOR runs. It is clear that the vector track prediction errors of the SYN-VOR run are much lower (168 km, 109 km, 332 km, 601 km and 126 km at 06, 12, 18, 24 and 30 hours of forecast) as compared to the CTRL run. However, the impact of the synthetic vortex reduces on and after 36 hours with higher track errors for the SYN-VOR run.

5. CONCLUSIONS

This study investigated the impact of inclusion of a NCAR-AFWA synthetic vortex scheme to a tropical cyclone which formed over the Bay of Bengal during November 2002. This is just one case study of a tropical cyclone, which formed over the Bay of Bengal during November 2002. It would be desirable to extend the scope of this study to several such tropical cyclones over India and obtain overall broad conclusions. The results of the study indicated that inclusion of the synthetic vortex has caused improvement in the simulation of wind asymmetries and warm temperature anomalies. The time series of the minimum SLP and MWS do reveal that the SYN_VOR run is closer to the observations than the CTRL run. The central minimum SLP and the MWS of the SYN-VOR run vortex are lower by 12 hPa and higher by 12 m sec $^{-1}$ as compared to the CTRL run. Improved overall structure of the wind and temperature fields have contributed to improved track prediction of the tropical cyclones with considerable reduction in the vector track prediction errors till 30 hours of forecast. The SYN-VOR run also simulates the structure in the spatial distribution of the precipitation pattern normally associated with a tropical cyclone. There are of course issues whether an axi-symmetric vortex of fixed size with a fixed maximum wind speed at a specified radius of maximum wind in nonlinear balance between the mass and wind fields is the best option of initializing a tropical cyclone. Also, the detailed structure of the boundary layer (whose role cannot be minimized) does not seem to be represented in the synthetic vortex formulation. It is envisaged that after prescribing the synthetic vortex and after some few hours of integration, the dynamics of the mesoscale model will ensure that the boundary layer and its dynamics play its rightful and important role. The ideal option for modifying the initial structure of the tropical cyclone should arise from availability of more observations

(satellite, buoys, ships, and drop sondes from instrumented aircraft through the vertical cross section of the tropical cyclone) in the cyclone vicinity together with accurate and high-resolution analysis rather than through inclusion of synthetic vortex.

ACKNOWLEDGEMENTS

MM5 model and NCEP-reanalysis data were obtained from NCAR, and NCEP. NCAR-AFWA synthetic vortex scheme was got from NCAR and AFWA. The authors thank the IMD for providing the observations regarding the intensity and track of the November 2002 Bay of Bengal tropical cyclone being investigated in this study. This work is supported under a research project funded by Department of Science and Technology, India and two of the authors (AC and SKD) thank DST for its support. One of the authors (S.Sandeep) acknowledges the CSIR, India for providing a research fellowship to carry out the present work.

REFERENCES

Davis, C.A., and Low-Nam. S. 2001, The NCAR-AFWA tropical cyclone bogussing Scheme. Air Force Weather Agency Report, NCAR Boulder, CO., 13 pp.

Grell, G.A., Dudhia, J., and Stauffer. D.R. 1994, A description of the fifth-generation Penn State/NCAR mesoscale model (MM5). NCAR Technical Note TN-398+STR National Center for Atmospheric Research Boulder CO., 122 pp.

Krishnamurti, T.N., Bedi, H.S., and Ingles. K. 1993, Physical initialization using SSM/I rain rates. Tellus, 45A**,** 247-269.

Kurihara, Y., Bender, M.A., and Ross. R.J. 1993, An initialization scheme of hurricane models by vortex specification. Monthly Weather Review, 121, 2030-2045.

Leslie, L.M., and Holland. G.J. 1995, On the bogussing of tropical cyclones in numerical models: A comparison of vortex profiles. Meteorology and Atmospheric Physics, 56, 101-110.

Mathur. M.B. 1991, The National Meteorological Center's quasi-Lagrangian model for hurricane prediction. Monthly Weather Review, 109, 1419-1447.

Mishra, D.K., and Gupta. G.R. 1976, Estimation of maximum wind speeds in tropical cyclones occurring in Indian Seas. Indian Journal of Meteorology, Hydrology & Geophysics, 27, 285-290.

Mohanty, U.C., Mandal, M., and Raman. S. 2004, Simulation of Orissa Super Cyclone (1999) using PSU/NCAR mesoscale model. Natural Hazards, 31, 373-390.

Prasad. K. 2005, Further experiments on cyclone track prediction with a quasi-Lagrangian limited area model. Meteorology and Atmospheric Physics, DOI 10.1007/s00703-004-0103-x, pp 17.

Rao, G.V., and Bhaskara Rao. D.V. 2003, A review of some observed mesoscale characteristics of tropical cyclones and some preliminary numerical simulations of their kinematic features. Proceedings of Indian National Science Academy, 69A, 523-541.

Roy Abraham, K., Mohanty, U.C., and Dash. S.K. 1995, Simulation of cyclones using synthetic data. Proceedings of Indian Academy of Sciences (Earth and Planetary Sciences), 104, 635-666.

Trivedi, D.K., Sanjay, J., and Singh. S.S. 2002, Numerical simulation of a super cyclonic storm, Orissa 1999: impact of initial conditions. Meteorological Application, 9, 367-376.

Table 1: Vector displacement track errors (km) with respect to observations

Time (hours)	Without-synthetic vortex	With-synthetic vortex
06	223	55
12	235	126
18	511	179
24	668	67
30	369	243
36	283	363
42	335	619

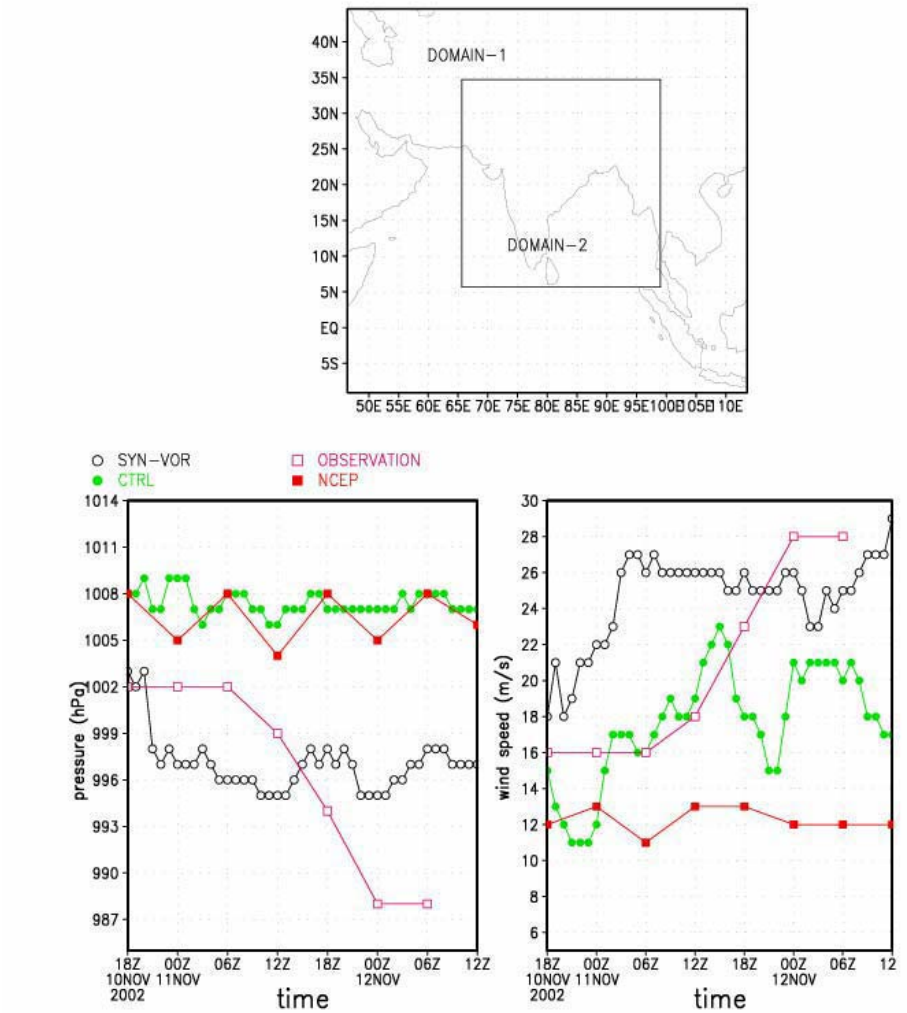

Figure 1: (a) MM5 model domain (90 km and 30 km grid spacing), (b) Time series of minimum SLP and (c) MWS. Filled circles and squares refer to CTRL run and NCEP reanalysis while unfilled circles and squares refer to SYN-VOR run and IMD observations

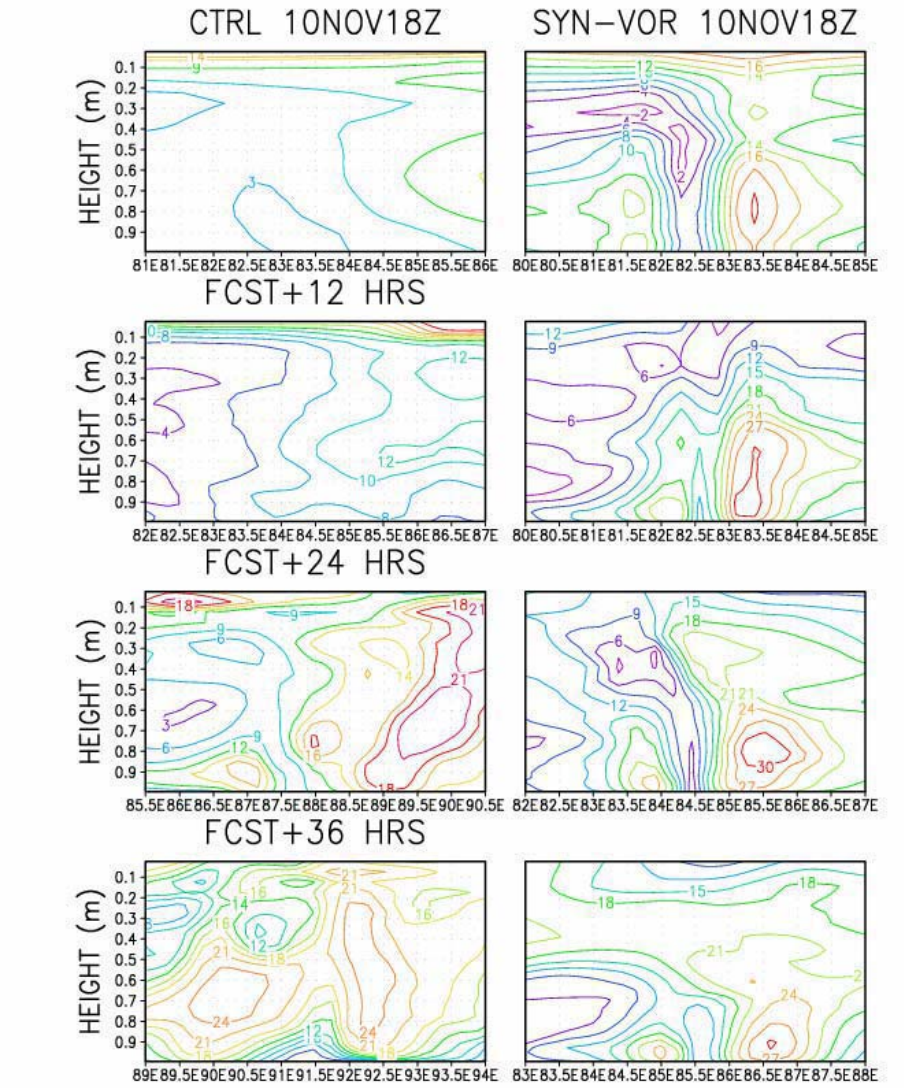

Figure 2: East-west cross section of the wind speed through the center of a cyclone at initial (10 November 2002 18 UTC), 12, 24 and 36 hours of forecast for CTRL (left panels) and SYN-VOR (right panels) runs.

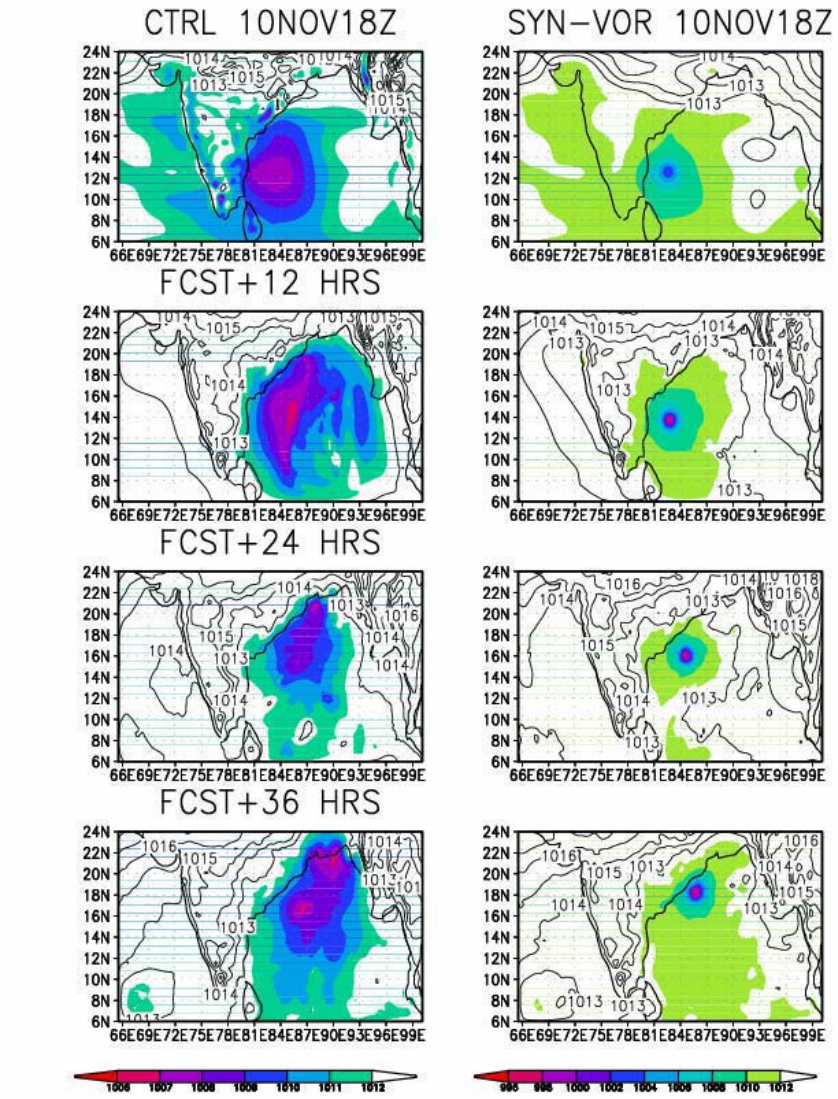

Figure 3: SLP at initial (10 November 2002 18 UTC), 12, 24 and 36 hours of forecast for CTRL (left panels) and SYN-VOR (right panels) runs.

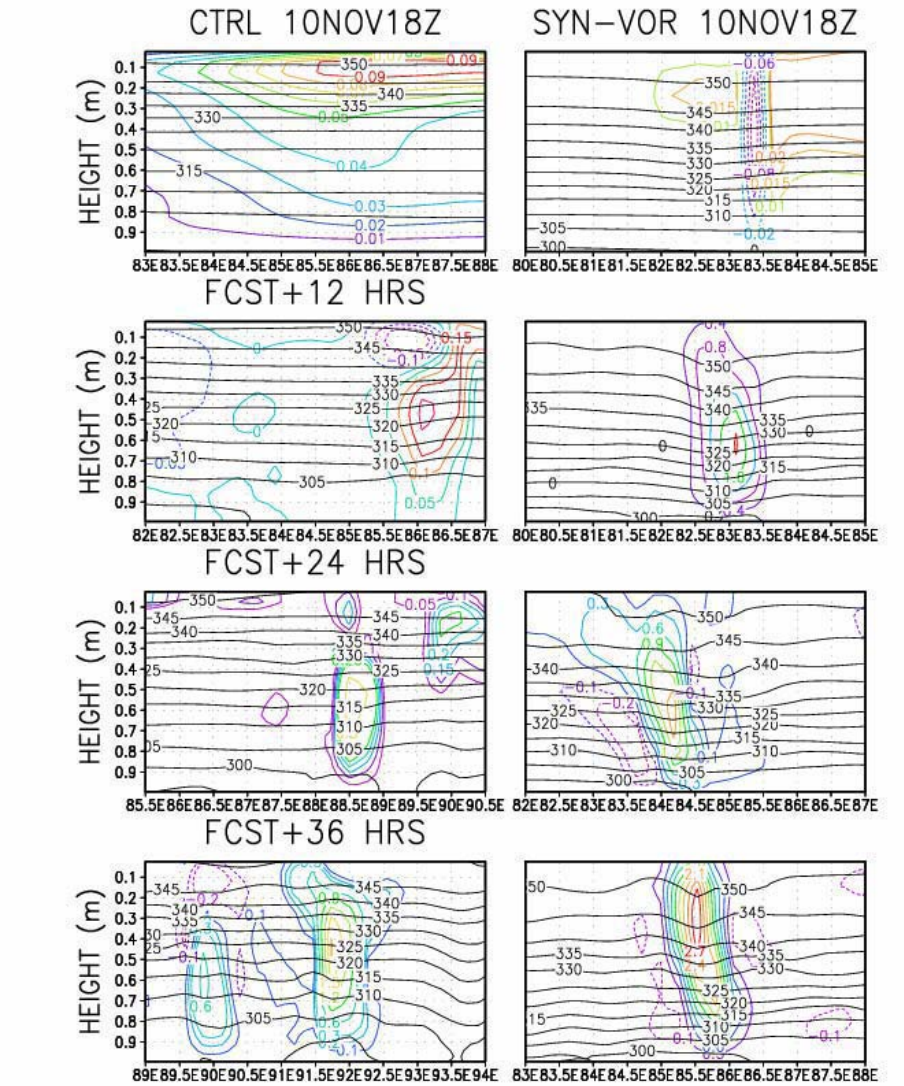

Figure 4: East-west cross section of the potential temperature and vertical velocity through the center of the tropical cyclone at initial (10 November 2002 18 UTC), 12, 24 and 36 hours of forecast for CTRL (left panels) and SYN-VOR (right panels) runs.

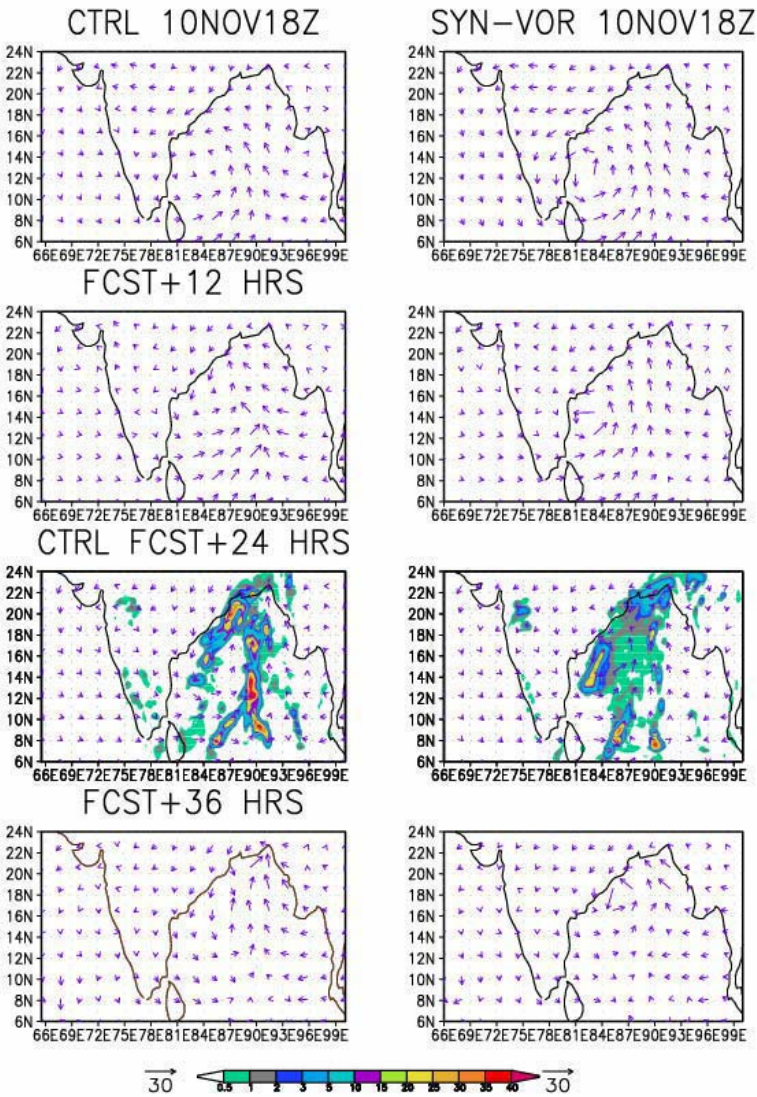

Figure 5: Lower tropospheric winds (m/s) (σ = 0.995 for CTRL and SYN-VOR runs) at initial (10 November 2002 18 UTC), 12, 24 and 36 hours of forecast for CTRL (left panels) and SYN-VOR (right panels) runs. Also has 24-hour accumulated precipitation (cm) for 11 November 2002 18 UTC for CTRL and SYN-VOR runs.

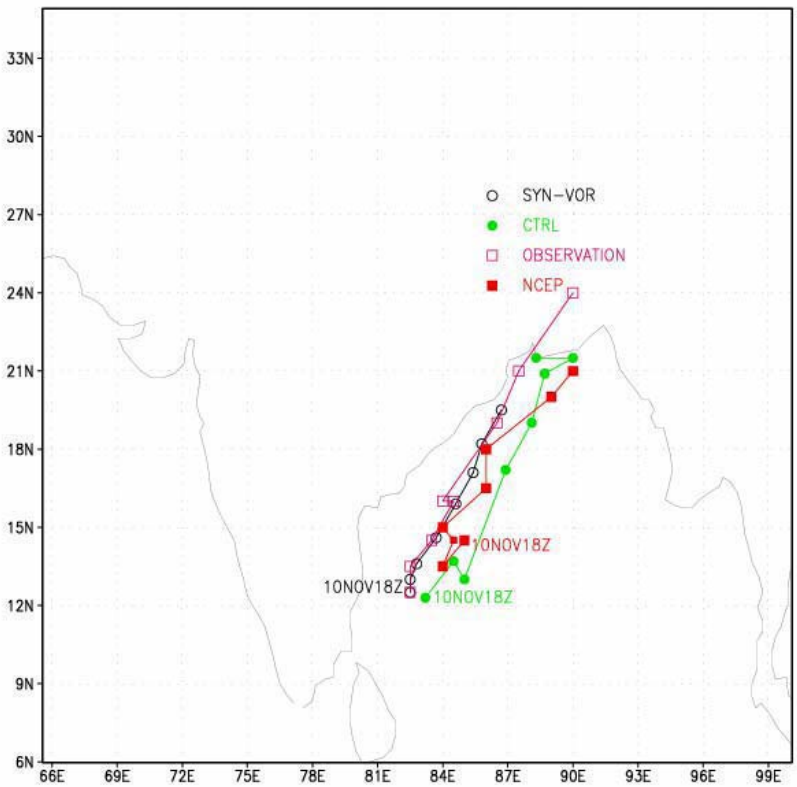

Figure 6: Track of cyclone in observations (unfilled square), NCEP reanalysis (filled square), SYN-VOR run (unfilled circle) and CTRL run (filled circle).

International Journal of Ecology & Development (IJED),
Winter 2006, Vol. 4, No. W06; Int. J. Ecol. Dev.; 52-65
ISSN 0972-9984; Copyright © 2006 IJED, ISDER

A Global Stability Result and Existence and Uniqueness of Solution to an Age-Structured SI Epidemic Model with Disease-Induced Mortality and Vertical Transmission of Disease

M. El-Doma

Faculty of Mathematical Sciences
University of Khartoum, P.O. Box: 321
Khartoum-Sudan

E-mail: biomath2004@yahoo.com

Abstract

We prove the existence and uniqueness of solution to an SI age-structured epidemic model for a vertically as well as horizontally transmitted disease when the fertility, natural mortality and disease-induced mortality rates depend on age and the force of infection of proportionate mixing assumption type. We also show that solutions of the model equations depend continuously on the initial age-distributions; and that the trivial equilibrium is globally stable, if the net reproduction rate is less than one.

Keywords: Age-structure; Epidemic; Existence; Uniqueness; Vertical transmission; Horizontal transmission; Stability; Continuous dependence on initial age-distributions.

MSC 2000: 45K05, 35A05,35B30, 35B45,35B65,35L60, 92D30, 92D25.

1. INTRODUCTION

Age-structured SI epidemic models are studied in several recent papers and books, for example, Hoppensteadt [20, 21], Busenberg [3], Cooke and Busenberg [9], Busenberg and Cooke [2, 4, 5], Louie et al. [23] and El-Doma [11 , 12, 15, 17]. The model described in [21] is quite general, in addition to chronological age it also assumes “class age” meaning time since entering the present state. But it does not incorporate vertical transmission, which is the passing of infection from parents to newborn offspring. This mode of transmission plays an important role in maintaining some diseases, for example, see [2]. In [18], several examples of vertically transmitted diseases are given. Mathematical models of vertically transmitted diseases are formulated and analyzed in Fine and Le Duc [19], Busenberg and Cooke [2, 4, 5], Cooke and Busenberg [9], Busenberg et al. [7], Regniere [25], El-Doma [11, 12, 14, 15, 16, 17], Busenberg and Hadeler [6], Anderson and May [1], Busenberg [3] and Cha et al. [8].

In El-Doma [15], we studied the same model as in this paper, and we determined the steady states and obtained some stability results. The same model but without vertical

transmission is studied in [12] and [23]. In [12], we proved the conjecture about the local stability of the endemic equilibrium given in [23]. Also, in [11] the same model but without death due to disease is studied.

In this paper, we prove the existence and uniqueness of solution to an SI age-structured epidemic model in which the disease is vertically as well as horizontally transmitted, horizontal transmission is the passing of infection through direct or indirect contact with infected individuals; and the fertility, natural mortality and the disease-induced mortality rates depend on age. We also show that solutions of the model equations depend continuously on the initial age-distributions. In addition, we show that the trivial equilibrium is globally stable if the net reproduction rate is less than one.

The organization of this paper is as follows: in section 2 we describe the model and obtain the model equations; in section 3 we prove the uniqueness of solution; in section 4 we prove the existence and uniqueness of solution as well as the continuous dependence on the initial age-distributions; in section 5 we prove the global stability of the trivial equilibrium.

2. THE MODEL

In this section, we consider an age-structured population of variable size exposed to a fatal communicable disease. The disease is both vertically and horizontally transmitted. We assume the following.

1. s(a,t) and i(a,t), respectively, denote the age-density for susceptibles and infectives of age a at time t. Then

   $\int_{a1}^{a_2} s(a,t)da$ = total number of susceptibles at time t of ages between a_1 and a_2,

   $\int_{a1}^{a_2} i(a,t)da$ = total number of infectives at time t of ages between a_1 and a_2.

   We assume that the total population consists entirely of susceptibles and infectives.

2. Let k(a,a') denotes the probability that a susceptible individual of age a is infected by an infective individual of age a'. We further assume that k(a,a') = k_1(a).k_2(a'), this is known as the proportionate mixing assumption (see Dietz and Schenzle [10]). Therefore, the horizontal transmission of the disease occurs according to the following rule:

   $$k_1(a)s(a,t)\int_0^\infty k_2(a')i(a',t)da',$$

   where k_1(a) and k_2(a) are bounded, nonnegative, continuous functions of a. The term $k_1(a)\int_0^\infty k_2(a')i(a',t)da$ is called "force of infection" and we let $\lambda(t) = \int_0^\infty k_2(a)i(a,t)da$.

3. The fertility rate $\beta(a)$ is a nonnegative, continuous, with compact support [0,A], (A ≥ 0). Therefore, the number of births of susceptibles per unit time is given by $s(0,t)=\int_0^\infty \beta(a)\left[s(a,t)+(1-q)i(a,t)\right]da, q\in[0,1]$ and q is the probability of vertically transmitting the disease, $i(0,t)=q\int_0^\infty \beta(a)i(a,t)da$, that is, all newborns from susceptibles are susceptible, but a portion q of newborns from infected parents are infective, i.e., they acquire the disease via birth (vertical transmission).
4. The natural death rate $\mu(a)$ is the same for susceptibles and infectives and $\mu(a)$ is a nonnegative, bounded, continuous and $\exists a_0 \in[0,\infty)$ such that

$$\mu(a)>\overline{\mu}>0\ \forall a>a_0 \text{ and } \mu(a_2)>\mu(a_1)\ \forall a_2>a_1>a_0.$$

5. The disease-induced death rate $\alpha(a)$ is a nonnegative, bounded and continuous function of $a\in[0,\infty)$.
6. The initial age distributions: $s(a,0)=s_0(a)$ and $i(a,0)=i_0(a)$ are continuous, nonnegative and integrable functions of $a\in[0,\infty)$.

These assumptions lead to the following system of nonlinear integro-partial differential equations with non-local boundary conditions, which describes the dynamics of the transmission of the disease.

$$\begin{cases}\dfrac{\partial s(a,t)}{\partial a}+\dfrac{\partial s(a,t)}{\partial t}+\mu(a)s(a,t)=-k_1(a)s(a,t)\lambda(t), a>0, t>0,\\ \dfrac{\partial i(a,t)}{\partial a}+\dfrac{\partial i(a,t)}{\partial t}+\mu(a)i(a,t)=k_1(a)s(a,t)\lambda(t)-\alpha(a)i(a,t), a>0, t>0,\\ s(0,t)=\int_0^\infty \beta(a)\left[s(a,t)+(1-q)i(a,t)\right]da, t\ge 0,\\ i(0,t)=q\int_0^\infty \beta(a)i(a,t)da, t\ge 0,\\ \lambda(t)=\int_0^\infty k_2(a)i(a,t)da, t\ge 0,\\ s(a,0)=s_0(a), i(a,0)=i_0(a), a\ge 0.\end{cases} \tag{2.1}$$

We note that problem (2.1) is an SI age-structured epidemic model, which has been studied in [15], where the steady states are determined and some stability results are obtained. The same model but with q = 0 (the case of no vertical transmission) is studied in [12] and [23] . Also, in [11] and [17] problem (2.1) is studied when $\alpha\equiv 0$.

In what fellows, we prove the existence and uniqueness of solution to problem (2.1), and we show that solutions of the model equations depend continuously on the initial age-distributions. In addition, we prove that the trivial equilirium is globally stable; this result generlizes the local stability result given in [23], for diseases without vertical transmission.

3. UNIQUENESS OF SOLUTION

In this section, we establish the uniqueness of solution to problem (2.1). First we prove a priori estimate, to that end, we assume that s(a,t) $\geq$ 0 and i(a,t) $\geq$ 0 and let p(a,t) = s(a,t) + i(a,t) and hence from (2.1) we find that p(a,t) satisfies the following:

$$\begin{cases} \dfrac{\partial p(a,t)}{\partial a}+\dfrac{\partial p(a,t)}{\partial t}+\mu(a)p(a,t)=-\alpha(a)i(a,t), a>0, t>0, \\ p(0,t)=B(t)=\displaystyle\int_0^\infty \beta(a)p(a,t)da, t\geq 0, \\ p(a,0)=p_0(a)=s_0(a)+i_0(a), a\geq 0. \end{cases} \tag{3.1}$$

From (3.1) we find that

$\dfrac{d}{dt}\displaystyle\int_0^\infty p(a,t)da \leq p(0,t) - \int_0^\infty \mu(a)p(a,t)da = \int_0^\infty (\beta(a)-\mu(a))p(a)da,$ and therefore, we obtain the following a priori estimate:

$$\int_0^\infty p(a,t)da \leq Me^{ct}, M=\int_0^\infty [s_0(a)+i_0(a)]da, c=\left\|\beta(a)-\mu(a)\right\|_\infty . \tag{3.2}$$

In order to prove uniqueness of solution to problem (2.1), we let (s^1(a,t), i^1(a,t)) and (s^2(a,t), i^2(a,t)) be two nonnegative solutions of problem (2.1) and we let $\zeta(a,t)$ = s^1(a,t) - s^2(a,t) and $\eta(a,t)$ = i^1(a,t) - i^2(a,t). Then $\omega(a,t)$ = $\zeta(a,t)$ + $\eta(a,t)$ satisfies the following:

$$\begin{cases} \dfrac{\partial \omega(a,t)}{\partial a}+\dfrac{\partial \omega(a,t)}{\partial t}+\mu(a)\omega(a,t)=-\alpha(a)\eta(a,t), a>0, t>0, \\ \omega(0,t)=\displaystyle\int_0^\infty \beta(a)\omega(a,t)da, t\geq 0, \\ \omega(a,0)=0, a\geq 0. \end{cases} \tag{3.3}$$

Using (3.3), we obtain:

$$\frac{d}{dt}\int_0^\infty |\omega(a,t)|da+\int_0^\infty \mu(a)|\omega(a,t)|da=\left|\int_0^\infty \beta(a)\omega(a,t)da\right|$$

$$-\int_0^\infty [sign\,\omega(a,t)]\alpha(a)\eta(a,t)da \leq \int_0^\infty \beta(a)|\omega(a,t)|da+\int_0^\infty \alpha(a)|\eta(a,t)|da.$$

And therefore, we obtain the following inequality:

$$\frac{d}{dt}\int_0^\infty |\omega(a,t)|da + \int_0^\infty \mu(a)|\omega(a,t)|da \le \int_0^\infty \beta(a)|\omega(a,t)|da + \int_0^\infty \alpha(a)|\eta(a,t)|da. \tag{3.4}$$

On the other hand from (2.1), we find that $\eta(a,t)$ satisfies the following:

$$\begin{cases} \dfrac{\partial\eta(a,t)}{\partial a} + \dfrac{\partial\eta(a,t)}{\partial t} + \mu(a)\eta(a,t) = k_1(a)s^1(a,t)\left(\displaystyle\int_0^\infty k_2(a')i^1(a,t)da\right) \\ -k_1(a)s^2(a,t)\left(\displaystyle\int_0^\infty k_2(a')i^2(a',t)da\right) - \alpha(a)\eta(a,t), a>0, t>0, \\ \eta(0,t) = q\displaystyle\int_0^\infty \beta(a)\eta(a,t)da, t\ge 0, \\ \eta(a,0) = 0, a \ge 0. \end{cases} \tag{3.5}$$

From (3.5), we obtain the following:

$$\frac{d}{dt}\int_0^\infty |\eta(a,t)|da + \int_0^\infty [\mu(a)+\alpha(a)]|\eta(a,t)|da = \left|q\int_0^\infty \beta(a)\eta(a,t)da\right|$$
$$+\left(\int_0^\infty k_2(a)i^1(a,t)da\right)\int_0^\infty k_1(a)[sign\,\eta(a,t)]s^1(a,t)da$$
$$-\left(\int_0^\infty k_2(a)i^2(a,t)da\right)\int_0^\infty k_1(a)[sign\,\eta(a,t)]s^2(a,t)da.$$

Note that $s^1(a,t) = \zeta(a,t) + s^2(a,t)$ and $i^2(a,t) = i^1(a,t) - \eta(a,t)$, therefore,

$$\frac{d}{dt}\int_0^\infty |\eta(a,t)|da + \int_0^\infty [\mu(a)+\alpha(a)]\,|\eta(a,t)|\,da \le q\int_0^\infty \beta(a)|\eta(a,t)|da$$
$$+\left(\int_0^\infty k_2(a)i^1(a,t)da\right)\int_0^\infty k_1(a)\,|\xi(a,t)|\,da + \left(\int_0^\infty k_2(a)\,|\eta(a,t)\,|da\right)\int_0^\infty k_1(a)s^2(a,t)da.$$

Noting that $|\zeta| \le |\omega| + |\eta|$ and using (3.2) for $i^1(a,t)$ and $s^2(a,t)$, we obtain

$$\frac{d}{dt}\int_0^\infty |\eta(a,t)|da + \int_0^\infty [\mu(a)+\alpha(a)]\,|\eta\,(a,t)|da \le \left[q\|\beta(a)\|_\infty + 2\|k_1(a)\|_\infty \|k_2(a)\|_\infty Me^{ct}\right]\times$$
$$\int_0^\infty |\eta(a,t)|da + \|k_1(a)\|_\infty \|k_2(a)\|_\infty Me^{ct}\int_0^\infty |\omega(a,t)|da, \tag{3.6}$$

where M and c are defined as in (3.2).

Setting $\phi(t) = \int_0^\infty |\omega(a,t)|da$ and $\psi(a,t) = \int_0^\infty |\eta(a,t)|da$, we find from (3.4) and (3.6) that $\phi(t)$ and $\psi(t)$ satisfy the following:

$$\begin{cases} \phi'(t) \le c\phi(t) + \|\alpha(a)\|_\infty \psi(t), \\ \phi(0) = 0. \end{cases} \tag{3.7}$$

$$\begin{cases} \psi'(t) \le M\|k_1(a)\|_\infty \|k_2(a)\|_\infty e^{ct}\phi(t) \\ +\left[q\|\beta(a)\|_\infty + 2\|k_1(a)\|_\infty \|k_1(a)\|_\infty Me^{ct} + \|\mu(a)+\alpha(a)\|_\infty\right]\psi(t), \\ \psi(0) = 0. \end{cases} \tag{3.8}$$

From (3.7) and (3.8), we get that $\phi(t) = \psi(t) = 0$, and therefore, $s^1(a,t) = s^2(a,t)$ and $i^1(a,t) = i^2(a,t)$. And hence, we have proved the following theorem:

Theorem (3.1). If Problem (2.1) has a solution $s(a,t) \ge 0$ and $i(a,t) \ge 0$, then it is unique.

4. EXISTENCE AND UNIQUENESS OF SOLUTION AND CONTINUOUS DEPENDENCE ON INITIAL AGE-DISTRIBUTIONS

In this section, we show that problem (2.1) has a unique solution that exists for all time. Furthermore, we show that solutions of problem (2.1) depend continuously on the initial age-distributions.

As in equation (3.2), we can deduce that p(a,t) satisfies the following inequality (also see [22]):

$$\int_0^\infty p(a,t)da \le \|p_0(a)\|_{L^1[0,\infty)} e^{(\|\beta(a)\|_\infty - \mu_*)t}, \tag{4.1}$$

where μ_* is given by

$$\mu_* = \inf_{a\in[0,\infty)} \mu(a). \tag{4.2}$$

Then using (3.1) and (4.1), we obtain that B(t) satisfies (also see [22])

$$B(t) \le \|\beta(a)\|_\infty \|p_0(a)\|_{L^1[0,\infty)} e^{(\|\beta(a)\|_\infty - \mu_*)t}. \tag{4.3}$$

Now, using (2.1), we obtain that s(a,t) and i(a,t) satisfy the following systems of equations:

$$\begin{cases} \dfrac{\partial s(a,t)}{\partial a} + \dfrac{\partial s(a,t)}{\partial t} + \mu(a)s(a,t) = -k_1(a)s(a,t)\lambda(t),\ a>0,\ t>0, \\ s(0,t) = B(t) - i(0,t), \quad t>0, \\ s(a,0) = s_0(a), \quad a \ge 0, \end{cases} \tag{4.4}$$

$$\begin{cases} \dfrac{\partial i(a,t)}{\partial a} + \dfrac{\partial i(a,t)}{\partial t} + [\mu(a)+\alpha(a)]i(a,t) = k_1(a)s(a,t)\lambda(t),\ a>0,\ t>0, \\ i(0,t) = q\displaystyle\int_0^\infty \beta(a)i(a,t)da,\ t>0, \\ i(a,0) = i_0(a), \quad a \ge 0, \\ \lambda(t) = \displaystyle\int_0^\infty k_2(a)i(a,t)da,\ t \ge 0. \end{cases} \tag{4.5}$$

By integrating problem (4.4) along characteristic lines t-a = const., we find that s(a,t) satisfies

$$s(a,t)=\begin{cases} s_0(a-t)e^{-\int_0^t[\mu(a-t+\tau)+k_1(a-t+\tau)\lambda(\tau)]d\tau}, & a>t, \\ [B(t-a)-i(0,t-a)]\pi(a)e^{-\int_0^a k_1(\tau)\lambda(t-a+\tau)d\tau}, & a<t, \end{cases} \tag{4.6}$$

where π(a) is given by

$$\pi(a)=e^{-\int_0^a \mu(c)dc}. \tag{4.7}$$

By integrating problem (4.5) along characteristic lines t-a = const., and using (4.6) we obtain that i(a,t) satisfies

$$i(a,t)=\begin{cases} e^{-\int_0^t[\mu(a-t+\tau)+\alpha(a-t+\tau)]d\tau}[i_0(a-t)+s_0(a-t)\int_0^t A(a-t,\sigma)d\sigma], & a>t, \\ i(0,t-a)\pi_2(a)+[B(t-a)-i(0,t-a)]\pi_2(a)\int_0^a D(t-a,\sigma)d\sigma, & a<t, \end{cases} \tag{4.8}$$

where $\pi_2(a), A(a-t,\sigma), D(t-a,\sigma)$ are given, respectively, by

$$\pi_2(a)=\pi(a)e^{-\int_0^a \alpha(\tau)d\tau}, \tag{4.9}$$

$$A(a-t,\sigma)=k_1(a-t+\sigma)e^{\int_0^\sigma[\alpha(a-t+\tau)-k_1(a-t+\tau)\lambda(\tau)]d\tau}\lambda(\sigma), \tag{4.10}$$

$$D(t-a,\sigma)=k_1(\sigma)e^{\int_0^\sigma[\alpha(\tau)-k_1(\tau)\lambda(t-a+\tau)]d\tau}\lambda(t-a+\sigma). \tag{4.11}$$

We notice that, since s_0(a), i_0(a) and p_0(a) are nonnegative, continuous and integrable functions, we can use (4.8) and (4.3) to show that,

$$\int_0^\infty i(t)da \le \|p_0(a)\|_{L^1[0,\infty)} e^{(\|\beta(a)\|_\infty-\mu_*)t}. \tag{4.12}$$

It is worth noting that if we can establish a solution for problem (4.5), then we can use this solution in (4.6) to show that (4.4) has a unique solution, whence the pair (s(a,t),i(a,t)) will determine the unique solution of problem (2.1). To establish the existence and uniqueness of solution to problem (2.1), we start by defining the following set E to satisfy:

E = {i(a,t): i(.,t) $\in$ L^1 ([0,∞); C[0,t_0]), a$\in$ [0,∞), t $\in$[0,t_0], |||i(a,t)||| = $\sup_{t\in[0,t_0]} \|i(a,t)\|_{L^1}$ },

where C[0,t_0] denotes the Banach space of continuous functions in [0,t_0], and $L^1[0,\infty)$ denotes the space of equivalent classes of Lebesgue integrable functions. We note that E is a Banach space.

In order to facilitate our future calculations, we need the following lemma.

Lemma (4.1). Suppose that x, y≥ 0, then $\left|e^{-y}-e^{-x}\right| \le |y-x|$.

Proof. Let $f(x)=e^{-x}$, then use the mean value theorem to establish the required result. In the next theorem, we prove the existence and uniqueness of solution to problem (2.1) via a fixed point theorem.

Theorem (4.1). Problem (2.1) has a unique solution that exists for all time.

Proof. Define the set Q by Q = {i(a,t) ∈ E, i(a,t) ≥ 0, ||| i(a,t)||| ≤ M}, where M is a constant which satisfies the following:

$$M > \|p_0(a)\|_{L^1} e^{(\|\beta(a)\|_\infty - \mu_*)t_0}. \tag{4.13}$$

We note that Q is a closed set in E. Now, for fixed initial-age distributions $s_0(a)$, $i_0(a)$ and $p_0(a)$, define the mapping T: Q⊂E→E by

$$Ti(a,t)=\begin{cases} e^{-\int_0^t [\mu(a-t+\tau)+\alpha(a-t+\tau)]d\tau} [i_0(a-t)+s_0(a-t)\int_0^t A(a-t,\sigma)d\sigma], & a>t, \\ i(0,t-a)\pi_2(a)+[B(t-a)-i(0,t-a)]\pi_2(a)\int_0^a D(t-a,\sigma)d\sigma, & a<t. \end{cases} \tag{4.14}$$

We note that by (4.12), we can see that T maps Q into Q. Now, we look for a fixed point of this mapping to provide existence and uniqueness of solution for problem (4.5). To this end, we let i(a,t) and i_1(a,t) be two elements of Q, and let $p(a,t)$ and $p_1(a,t)$ be the corresponding solutions of problem (3.1). Then by using (3.1), we can obtain the following inequality:

$$\| p(.,t) - p_1(.,t) \|_{L^1} \le \| \alpha(a) \|_\infty e^{\|\beta(a)\|_\infty t_0} \int_0^t \|i(.,\sigma) - i_1(.,\sigma)\|_{L^1} d\sigma. \tag{4.15}$$

Then using (4.15), (4.3), (4.12), and lemma (4.1), we obtain

$$\|Ti(.,t) - Ti_1(.,t)\|_{L^1} \le K(M,t_0)\int_0^t \|i(.,\sigma) - i_1(.,\sigma)\|_{L^1} d\sigma, \tag{4.16}$$

where K(M, t_0)is a constant which depends on M and t_0. Therefore,

$$|||Ti(.,t)-Ti_1(.,t)||| \le t_0\, K(M,t_0)\, ||| i(.,\sigma) - i_1(.,\sigma) |||. \tag{4.17}$$

And thus, by induction, for each positive integer n, we obtain

$$|||\, T^n i(.,t) - T^n i_1(.,t)\,||| \le \frac{[\,t_0\, K(M,t_0)]^n}{n!}\,|||\, i(.,t) - i_1(.,t)\,|||. \tag{4.18}$$

Inequality (4.18) implies that there exists a positive integer N such that T^N is a strict contraction on Q. Thus T has a unique fixed point in Q. Since t_0 is arbitrary, it follows that problem (4.5) has a unique solution that exists for all time. Now, we can use this solution in (4.6) and observe that s(a,t) satisfies (4.12). Whence similar arguments, as before, will determine the unique solution of system (4.4). Therefore, the pair (s(a,t),i(a,t)) will determine the unique solution of problem (2.1). This completes the proof of the theorem.

In the next theorem, we show that solutions of problem (2.1) depend continuously on the initial age-distributions, therefore, problem (2.1) is well posed.

Theorem(4.2). Let p(a,t) and p_1(a,t) be two solutions of problem (3.1) corresponding to initial age-distributions p_0(a), s_0(a), i_0(a) and p_{01}(a), s_{01}(a), i_{01}(a), respectively. Also, suppose that p(0,t)= B(t) and p_1(0,t) = B_1(t), and let i(a,t) and i_1(a,t) be the corresponding solutions of problem (4.5). If $K_0(M,t_0), K(M,t_0)$ are constants that depend on M and t_0 then the following properties hold:

$$\|\, p(.,t) - p_1(.,t)\,\|_{L^1} \le \|\, p_0(a) - p_{01}(a)\,\|_{L^1}\, e^{(\|\beta(a)\|_\infty - \mu_*)t} + \|\alpha(a)\|_\infty\, e^{\|\beta(a)\|_\infty t_0} \int_0^t \|i(.,\sigma) - i_1(.,\sigma)\|_{L^1}\, d\sigma, \tag{4.19}$$

$$|\, B(t) - B_1(t)\,| \le \|\beta(a)\|_\infty\, \|\, p(.,t) - p_1(.,t)\,\|_{L^1}\,, \tag{4.20}$$

$$\begin{aligned} &\|\, i(.,t) - i_1(.,t)\,\|_{L^1} \le \\ &\Big[\, \|\, s_0(a) - s_{01}(a)\,\|_{L^1} + \|\, i_0(a) - i_{01}(a)\,\|_{L^1} + \|\, p_0(a) - p_{01}(a)\,\|_{L^1} \,\Big] e^{\|\beta(a)\|_\infty t_0}\, e^{tK(M,t_0)}, \end{aligned} \tag{4.21}$$

$$\begin{aligned} \|\, s(.,t) - s_1(.,t)\,\|_{L^1} \le{}& \|\, s_0(a) - s_{01}(a)\,\|_{L^1} + \|\, p_0(a) - p_{01}(a)\,\|_{L^1}\, e^{\|\beta(a)\|_\infty t_0} + \\ & K_0(M,t_0) \int_0^t \|i(.,\sigma) - i_1(.,\sigma)\|_{L^1}\, d\sigma. \end{aligned} \tag{4.22}$$

Proof. Note that (4.19) can be proved in a similar way as (4.15), and that (4.20) follows from (3.1) and (4.19). Now, to obtain (4.21), we first use (4.8), and then use (4.16), (4.19), (4.20) to obtain the following:

$$\begin{aligned} \|\, i(.,t) - i_1(.,t)\,\|_{L^1} \le{}& \Big[\, \|\, s_0(a) - s_{01}(a)\,\|_{L^1} + \|\, i_0(a) - i_{01}(a)\,\|_{L^1} + \|\, p_0(a) - p_{01}(a)\,\|_{L^1}\, e^{\|\beta(a)\|_\infty t_0} \,\Big] \\ & + K(M,t_0) \int_0^t \|\, i(.,\sigma) - i_1(.,\sigma)\,\|_{L^1}\, d\sigma. \end{aligned}$$

Now, the foregoing inequality yields (4.21) by the aid of Gronwall's inequality. By using (4.6), (4.12), (4.19) and (4.20), we obtain (4.22). This completes the proof of the theorem.

We note that (4.19)-(4.22) show that solutions of problem (2.1) depend continuously on the initial age-distributions, and therefore, problem (2.1) is well posed.

Also, note that in order to obtain a solution that is differentiable (C^1), we need the following compatibility conditions:

$$\begin{aligned} s_0'(0) &= -q\left(\int_0^\infty k_2(a)i_0(a)da\right)\int_0^\infty \beta(a)k_1(a)s_0(a)da \\ &\quad -\int_0^\infty \beta(a)\left[(1-q)((\alpha(a)+\mu(a))i_0(a)+i_0'(a))+\mu(a)s_0(a)+s_0'(a)\right]da \\ &= -\left[\mu(0)s_0(0)+k_1(0)s_0(0)\left(\int_0^\infty k_2(a)i_0(a)da\right)+s_0'(0)\right], \end{aligned} \tag{4.23}$$

$$s_0(0) = \int_0^\infty \beta(a)\left[s_0(a)+(1-q)i_0(a)\right]da, \tag{4.24}$$

$$\begin{aligned} i_0'(0) &= q\left(\int_0^\infty k_2(a)i_0(a)da\right)\int_0^\infty \beta(a)k_1(a)s_0(a)da \\ &\quad -q\int_0^\infty \beta(a)\left[(\alpha(a)+\mu(a))i_0(a)+i_0'(a)\right]da \\ &= k_1(0)s_0(0)\left(\int_0^\infty k_2(a)i_0(a)da\right)-\left[\mu(0)+\alpha(0)\right]i_0(0)-i_0'(0), \end{aligned} \tag{4.25}$$

$$i_0(0) = q\int_0^\infty \beta(a)i_0(a)da. \tag{4.26}$$

5. GLOBAL STABILITY OF THE TRIVIAL EQUILIBRIUM

In this section, we study the stability of the trivial steady state for problem (2.1). It is worth noting that in [15], the steady states for problem (2.1) are determined, and some stability results are obtained. Also, we note that in [15], it is shown that if the net reproduction rate $R_0 = \int_0^\infty \beta(a)\pi(a)da < 1,$ then the only steady state for problem (2.1) is the trivial equilibrium: s(a,t) = i(a,t) = 0.

By integrating problem (3.1) along characteristics lines t - a = constant, we find that p(a,t) satisfies

$$p(a,t) = \begin{cases} p_0(a-t)\exp\left(-\int_0^t\left[\mu(a-t+\tau)+\alpha(a-t+\tau)\right]d\tau\right)+ \\ \int_0^t \exp\left(-\int_\sigma^t\left[\mu(a-t+\tau)+\alpha(a-t+\tau)\right]d\tau\right)\alpha(a-t+\sigma)s(a-t+\sigma,\sigma)d\sigma, a>t, \\ \\ B(t-a)\pi_2(a)+\int_0^a \exp\left(-\int_\sigma^a\left[\mu(\tau)+\alpha(\tau)\right]d\tau\right)\alpha(\sigma)s(\sigma,t-a+\sigma)d\sigma, a<t. \end{cases} \tag{5.1}$$

From (3.1) and (5.1), we find that B(t) satisfies

$$B(t) = \int_0^t h(a)B(t-a)da + \int_0^t \int_0^\infty \beta(a+\sigma)\exp(-\int_a^{a+\sigma}[\mu(\tau)+\alpha(\tau)]d\tau)\alpha(a)s(a,t-\sigma)dad\sigma +$$

$$\int_t^\infty \beta(a)\exp(-\int_a^{a+\sigma}[\mu(a-t+\tau)+\alpha(a-t+\tau)]d\tau)p_0(a-t)da. \tag{5.2}$$

Where h(a) is defined as follows

$$h(a) = \beta(a)\pi_2(a). \tag{5.3}$$

From (4.5) and (4.8), we find that $\lambda(t)$ satisfies

$$\lambda(t) = \int_0^t \int_0^\infty k_2(a+\sigma)\exp(-\int_a^{a+\sigma}[\mu(\tau)+\alpha(\tau)]d\tau)k_1(a)s(a,t-\sigma)\lambda(t-\sigma)dad\sigma +$$

$$\int_t^\infty k_2(a)i_0(a-t)\exp(-\int_0^t[\mu(a-t+\tau)+\alpha(a-t+\tau)]da + \int_0^t f(a)i(0,t-a)da. \tag{5.4}$$

Where f is defined as follows

$$f(a) = k_2(a)\pi_2(a). \tag{5.5}$$

Setting $i(0,t) = V(t)$ and using (4.5), (4.8) and (4.6) we obtain that $V(t)$ satisfies

$$\begin{aligned} V(t) &= q\int_0^t h(a)V(t-a))da + \\ &q\int_0^t\int_0^\infty \beta(a+\sigma)\exp(-\int_a^{a+\sigma}[\mu(\tau)+\alpha(\tau)]d\tau)k_1(a)s(a,t-\sigma)\lambda(t-\sigma)dad\sigma \\ &+ q\int_t^\infty \beta(a)i_0(a-t)\exp(-\int_0^a[\mu(a-t+\tau)+\alpha(a-t+\tau)]d\tau)da. \end{aligned} \tag{5.6}$$

We note that by assumption (3), (4), and (6) of section (2), and the dominated convergence theorem that

$$\int_t^\infty \beta(a)p_0(a-t)\exp(-\int_0^t[\mu(a-t+\tau)+\alpha(a-t+\tau)]d\tau)\ da \to 0,\ as\ t\to\infty.$$

Also, by the same reasoning as above,

$$\int_t^\infty k_2(a)i_0(a-t)\exp(-\int_0^t[\mu(a-t+\tau)+\alpha(a-t+\tau)]d\tau)\ da \to 0,\ as\ t\longrightarrow\infty \text{ and}$$

$$q\int_t^\infty \beta(a)i_0(a-t)\exp(-\int_0^t[\mu(a-t+\tau)+\alpha(a-t+\tau)]d\tau)\ da \to 0,\ as\ t\to\infty.$$

Consequently, B(t), $\lambda(t)$, and $V(t)$ satisfy the following limiting equations (see Miller [24]):

$$B(t) = \int_0^{\infty} h(a)B(t-a)da$$
$$+ \int_0^{\infty}\int_0^{\infty} h(a+\sigma)\left[B(t-a-\sigma) - V(t-a-\sigma)\right]J_{\alpha}(a)\exp(-\int_0^{a} k_1(\tau)\lambda(t-a-\sigma+\tau)d\tau)dad\sigma, \tag{5.7}$$

$$\lambda(t) = \int_0^{\infty} f(a)V(t-a)da + \int_0^{\infty}\int_0^{\infty} f(a+\sigma)J_{k_1}(a)[B(t-a-\sigma) - V(t-a-\sigma)]\times$$
$$\exp(-\int_0^{a} k_1(\tau)\lambda(t-a+\sigma+\tau)d\tau)\lambda(t-\sigma)dad\sigma, \tag{5.8}$$

$$V(t) = q\int_0^{\infty} h(a)V(t-a)da + q\int_0^{\infty}\int_0^{\infty} h(a+\sigma)[B(t-a-\sigma) - V(t-a-\sigma)]\times$$
$$J_{k_1}(a)\exp(-\int_0^{a} k_1(\tau)\lambda(t-a-\sigma+\tau)d\tau)\ \lambda(t-\sigma)dad\sigma. \tag{5.9}$$

Where J_{υ} is defined as follows

$$J_{\upsilon}(\sigma) = \upsilon(\sigma)\exp\left(\int_0^{\sigma}\alpha(\tau)d\tau\right). \tag{5.10}$$

In the following theorem, we show that the trivial equilibrium: i(a,t) =0, s(a,t)=0, is globally stable when $R_0 < 1,$

Theorem (5.1). Suppose that $R_0 < 1,$ then the trivial equilibrim: s(a,t) = 0, i(a,t) = 0, is globally stable.

Proof. Let $B^{\infty} = \limsup_{t\to\infty} B(t), \lambda^{\infty} = \lim_{t\to\infty}\lambda(t), V^{\infty} = \limsup_{t\to\infty} V(t),$ then from (5.7) and using Fatou's Lemma, we obtain the following:

$$B^{\infty} \le B^{\infty}\left[\frac{\int_0^{\infty}\int_0^{\infty} h(a+\sigma)J_{\alpha}(a)dad\sigma}{1-R(\alpha)}\right] < B^{\infty},$$ which is absurd unless $B^{\infty} = 0.$

From (5.9) and using Fatou's Lemma, we find that $V^{\infty} \le qR(\alpha)V^{\infty} < V^{\infty},$ which is absurd unless $V^{\infty} = 0.$ Now, using (5.8), we conclude that $\lambda^{\infty} = 0.$ Accordingly the trivial equilibrium is globally stable. This completes the proof of the theorem.

We remark that Theorem (5.1) can be proved directly using problem (3.1) by observing that p(a,t) must satisfy the following inequality:

$$p(a,t) \le \begin{cases} p_0(a-t)\pi(a)/\pi(a-t), & a > t, \\ B(t-a)\,\pi(a), & a < t. \end{cases} \tag{5.11}$$

Then from (5.11) and (3.1), we obtain that

$$B(t) \le \int_0^\infty \beta(a)\pi(a)B(t-a)da + be^{-\mu_* t}, \tag{5.12}$$

where b is a constant. And hence, from (5.12), we obtain that $B^\infty = 0,$ and accordingly, from (5.11), $p(a,t) \to 0,$ as $t \to \infty.$

Acknowledgements

The author would like to thank Professor Philippe Benilan for stimulating discussions. The author would also like to thank Professor Mimmo Iannelli, Professor Herbert W. Hethcote, Professor Horst R. Thieme, Professor G. C. Wake, Professor K. Dietz, Professor Michel Langlais, Professor Carlos Castillo-Chavez, and Professor Andrea Pugliese, for sending him references.

This paper was completed while the author was visiting the " Center for Advanced Mathematical Sciences" CAMS, at the American University of Beirut, Lebanon, and he wishes to express his gratitude for the hosbitality at the Center during his stay.

This research was supported in part by " The Third World Academy of Sciences" (TWAS), under Research Grant Agreement No. 98-364 RG/MATHS/AF/AC.

REFERENCES

[1] Anderson, R. M., and May, R. M., 1982, Directly transmitted infectious diseases: Control by vaccination. Science, 215, 1053-1060.

[2] Busenberg, S. N., and Cooke, K. L., 1993, Vertically transmitted diseases. Models and Dynamics. In Biomathematics Vol. 23, Springer-Verlag, Berlin.

[3] Busenberg, S. N., 1986, Age dependence and vertical transmission of diseases. 1986, J. Modelling of Biomedical Systems. 239-242.

[4] Busenberg, S. N., and Cooke, K. L., 1982, Models of Vertically transmitted diseases with sequential-continuous dynamics. In Lakshmikantham, V., (Eds), Nonlinear Phenomena in Mathematical Sciences Academic Press, New York.

[5] Busenberg, S. N., and Cooke, K. L., 1988, The population dynamics of two vertically transmitted infections. Theoretical Population Biology, Vol. 33, No. 2, 181-198.

[6] Busenberg, S. N., and Hadeler, K. P., 1990, Demography and epidemics. J. Math. Biosciences, 101, 63-74.

[7] Busenberg, S. N., and Cooke, K. L., and Pozo, M. A., 1983, Analysis of a model of a vertically transmitted disease. J. Math. Biology, 17, 305-329.

[8] Cha, Y., Iannelli, M., Milner, F., 1998, Existence and uniqueness of endemic states for the age-structured S-I-R epidemic model. Math. Biosci., Vol. 150, (1998), 177-190.

[9] Cooke, K. L., and Busenberg, S. N., 1983, Vertically transmitted diseases. In Lakshmikantham, V., (Eds), Nonlinear Phenomena in Mathematical Sciences, Academic Press, New York.

[10] Dietz, K., and Schenzle, D., 1985, Proportionate mixing models for age-dependent infection transmission. J. Math. Biol., 22, 117-120.

[11] El-Doma, M., 1987, Analysis of nonlinear integro-differential equations arising in age-dependent epidemic models. Nonlinear Analysis TMA, Vol. 11, 913-937.

[12] El-Doma, M., 2000, Analysis of an Age-Dependent SI Epidemic Model with Disease-Induced Mortality and Proportionate Miing Assumption. International Journal of Applied Mathematics, Vol. 3, No. 3, 233-247.

[13] El-Doma, M., 2000, Stability analysis of a general age-dependent vaccination model for a vertically transmitted disease under the proportionate mixing assumption. IMA J. Math. Appl. Med. Biol.,

17, 119-136.

[14] El-Doma, M., 1995, Analysis of a General Age-Dependent Vaccination Model for a Vertically Transmitted Disease. Nonlinear Times and Digest, Vol.2, 147-172.

[15] El-Doma, M., 2004, Analysis of an Age-Dependent SI Epidemic Model with Disease-Induced Mortality and Proportionate Mixing Assumption: The case of Vertically Transmitted Diseases. Journal of Applied Mathematics 2004: 3, 235-253.

[16] El-Doma, M., March-April 2005, Stability Analysis for an SIR Age-Structured Epidemic Model with Vertical Transmission and Vaccination. International Journal of Ecology & Development (IJED), Vol. 3, No. MA05, 1-38.

[17] El-Doma, M. 2004, Analysis of an age-structured epidemic model with vertical trnsmission and proportionate mixing assumption. MATH. SCI. RES. J., 8(8), 239-260.

[18] Fine, P. E. M., 1979, Vectors and vertical transmission: an epidemiologic perspective. Annals N. Y. Academic Sci., 266, 173-194.

[19] Fine, P. E. M., and Le Duc, J. W., 1978, Towards a quantitative understanding of the epidemiology of keystone virus in the Eastern United States. American J. Trop. Med. Hyg., 27, 322-338.

[20] Hoppensteadt, F., 1975, Mathematical Theory of population demographic, genetics and epidemics. CBMS-NSF regional Conference in applied Mathematics, Philadelphia.

[21] Hoppensteadt, F., 1974, An age-dependent epidemic model. J. Franklin Inst., 297, 325-333.

[22] Iannelli, M., 1995, Mathematical theory of age-structured population dynamics. CNR Applied Mathematics Monograph 7, Giardini Ed., Pisa, Italy.

[23] Louie, K., and Roberts, M. G., and Wake, G. C., 1994, The regulation of an age-structured population by a fatal disease. IMA J. Math. Appl. Med. & Biol., Vol. 11, 229-244.

[24] Miller, R. K., 1971, Nonlinear Volterra Integral Equations. W. A. Benjamin, Inc., Menlo Park , California.

[25] Regniere, J., 1984, Vertical transmission of diseases and population dynamics of insects with discrete generations. J. Theor. Biol. 107, 287-301.

International Journal of Ecology & Development (IJED),
Winter 2006, Vol. 4, No. W06; Int. J. Ecol. Dev.; 66-85
ISSN 0972-9984; Copyright © 2006 IJED, ISDER

Particle Swarm Optimisation Techniques for Deriving Operation Policies for Maximum Hydropower Generation: A Case Study

C. R. Suribabu

School of Civil Engineering,
SASTRA Deemed University,
Thanjavur, Tamilnadu, India

ABSTRACT

Planning the operation of reservoir for optimal power generation is important, due to uncertainty in future inflows and energy demand. The national interest in generating the hydroelectric power has focused on the potential for greater energy production from existing and planned reservoir systems. Determining the optimal long-term operation of a reservoir and assessing its potential towards various purposes for which it is intended, has been attempted by applying operation research techniques. A model for optimal operating policy of a reservoir for power generation using Particle swarm algorithm is developed. The focus of this paper is to assess the power generation potential of Indirasagar reservoir across the river Narmada in central part of India by Particle swarm optimisation (PSO) technique. This paper describes the monthly hydropower generation optimisation model to maximize the hydropower. The simulated results of the model show that the PSO is most promising and competitive and can be used for reservoir operation.

Key Words: *Hydroelectric power, operation research, particle swarm optimisation, reservoir operation.*

INTRODUCTION

A major research focus of the past five decades in water resources engineering has been on developing and adapting system analysis techniques for application in reservoir management and operations. A primary emphasis of systems analysis related to reservoir problems is the application of mathematical simulation and optimisation models to provide an improved basis for decision-making. Yeh (1985) provides a state of the art review of theories and applications of system analysis techniques to the reservoir problems. Algorithms and methods surveyed in this research include linear programming, dynamic programming, non-linear programming, and simulation. Many of these methods are included in textbooks like Loucks et al (1981). Simonovic (1992) provides short reviews of the mathematical models used in reservoir management and operations in support of previous state of

the art and provide two ideas for closing gap between theory and practice. A simple simulation – optimisation model for reservoir sizing and knowledge-based technology with regard to single-multiple reservoir analysis had illustrated with examples. Recently Labadie (2004) presented state art review on optimal operation of multi reservoir systems. Labadie (2004) viewed reservoir system optimisation problem in two general perspectives as traditional methods and non-traditional methods of optimisation. Algorithms and methods surveyed in this research include implicit stochastic optimisation (ISO), explicit stochastic optimisation models (ESO), multiobjective optimisation models and heuristic optimisation model. The review highlights the need of application of heuristic methods to overcome computational challenges of explicit stochastic optimisation, use of fuzzy rule based systems and neural networks to alleviate problem encountering to derive operating policies through implicit stochastic optimisation models and ability of genetic algorithms to get into with simulation models. Dynamic programming has been the popular techniques in the past for optimal operation (Stedinger et al, 1984; Gygier and Stedinger, 1985; Tejada-Guibert et al, 1995). Advantages of DP are its ability to address the non-linearities in the problem formulation, and to decompose complex problems. Use of genetic algorithm in determining the optimal reservoir operating policy has not received significant attention from water resources engineers, though Oliveira and Loucks (1997) and Wardlaw and sharif (1999) explored the potential of GA in reservoir operation. Huang (2001) has proposed Ant colony system based optimisation approach for the enhancement of hydroelectric generation scheduling. Ndiritu (2003) presented a multi-population genetic algorithm to optimise a system of two reservoirs that supplies monthly varying demands and environmental flow requirements. Optimisation aimed at minimising the penalty resulting from non-supply of water and the occurrence of low reservoir storage states that would inhabit non-consumptive water utilisation. Ahmed and Sarma (2004) used genetic algorithm model to find the operating policy of a multi purpose reservoir and compared with the results of discrete stochastic dynamic programming models. This paper is aimed at demonstrating the application of particle swarm optimisation technique to optimise the power generation from Indirasagar reservoir in view of arriving optimal operating policy.

PARTICLE SWARM OPTIMIZATION (PSO)

Particle swarm optimization is an evolutionary computation technique developed by Kennedy and Eberhart (1995) to model naturally occurring swarming behavior in a computer program. A particle represents a bird or bee or fish, or any other type of natural agent that exhibits swarming behavior. PSO as an optimization tool provides

a population based search procedure. A swarm or population consists of individuals, called particles and each particle represents a possible solution to the problem in hand. These potential solutions are flown in a multidimensional search space to determine the optimum position of them. This optimum position is usually characterized by optimum of a fitness function. All particles have velocities that direct the flying of the particles. All particles have fitness values, which are evaluated by a predefined fitness function that is to be optimized. Each particle keeps track of its coordinates in the problem space, which are associated with the best solution (fitness) it has achieved so far in its history. During flight each particle adjusts its position based on its own experience and according to the experience of others particles in the swarm, making use of the best position encountered by itself in the history of flying and the best position of other particles in the present state. As a consequence the particles move towards the global best solution.

As a particle moves through the search space, it compares its fitness value it has ever attained at any time up to current time and the best position so far is called individual best or local best. The local best reflects the cognition component of PSO. Global best is the best position among all individual best positions achieved so far and is usually called the social component of PSO. To a simple PSO model originally proposed Shi and Eberhart (1998) introduced an inertia weight to improve the convergence and speed of convergence. The inertia weight is employed to control the influence of the previous history of velocities on the current velocity, thus to influence the trade-off between global (widespread) and local (narrow) exploration abilities of the 'flying points'. A larger inertia weight facilitates global exploration (searching new areas) while a smaller inertia weight tends to facilitate local exploration to fine-tune the current search area. Suitable selection of the inertia weight can provide a balance between global and local exploration abilities and thus reduces the number of iterations required to reach the optimum. Thus the inertia weight helps to generate non-dominated solutions and maintains diversity. Particle is a candidate solution represented by i-dimensional vector, where i is the number of decision variables. Population is set of j particles at time t. PSO randomly initializes the position and velocity of each particle within the swarm at the beginning of the optimization. The position of the particles is updated in the following manner:

$$x_{t+1}^{i} = x_{t}^{i} + v_{t+1}^{i} \tag{1}$$

with the velocity v^{j} calculated as follows:

$$v_{t+1}^{i} = v_{t}^{i} + c_1 r_1 (p_{t}^{i} - x_{t}^{i}) + c_2 r_2 (p_{t}^{g} - x_{t}^{i}) \tag{2}$$

here, subscript t indicates an (unit) pseudo-time increment. p_t^i represents the best ever position of particle i at time t, with p_t^g representing the global best position in the swarm at time t. r_1 and r_2 represent uniform random numbers between 0 and 1. c_1 and c_2 represents the inertia weights which controls the impact of the previous velocities on the current velocity. Hence, it influences the trade-off between the global and local exploration abilities of the particles.

The initial swarm is created such that the particles are randomly, distributed throughout the design space, using a uniform distribution, each with a random initial velocity vector. The random initial position and velocity vectors are obtained from

$$x_0^i = x_{\min} + r_3(x_{\max} - x_{\min}) \quad (3)$$

$$v_0^i = \omega_1 x_0^i + \varpi_2 r_0(p_o^g - x_0^i) \quad (4)$$

The flowchart showing the steps of PSO is presented in Figure 1.

NARMADASAGAR COMPLEX

Narmadasagar Complex comprises of Indirasagar, Omkareshwar and Maheshwar projects across Narmada river in series from upstream to downstream. Indira sagar reservoir, being the main storage, would provide positive benefits of power generation, irrigation, domestic and industrial water supply and regulated releases down stream for further storage and utilization. The salient features of Indira Sagar reservoir considered for modeling are:

Minimum Draw down level (MDDL)	-	243.20 m
Reservoir capacity at MDDL	-	2470 Mm^3
Full reservoir level (FRL)	-	262.13 m
Reservoir Capacity at FRL	-	12222 Mm^3
Installed capacity	-	1000 MW
Tail water level	-	196.90 m

The active capacity of the reservoir is 9750 Mm^3.

The dam is proposed to be 92 m (302 Ft.) high and 653 m (2142 ft.) in length with a slightly curved alignment of 880 m radius across river Narmada near village Narmada Nagar of Development Block Punasa of the district about 845 Kms. from

the source of origin with a gross storage of 12.22 Bm^3 and a live storage of 9.75 Bm^3.

A sub surface powerhouse on the right bank is proposed to house 8 units of 125 MW each with conventional Francis Turbines. For present study, the available inflow data for a period of 32 years (1948-49 to 1979-80) is used for assessing the potential of power generation. The water year starts from July to June.

OPTIMIZATION MODEL

The optimization model is developed for monthly operation of reservoir so as to maximize the total power generation subjected to the following constraints

FLOW CONTINUITY EQUATION

The water balance per month based on the principle of conservation of mass is given by

$$S_t = S_{t-1} + I_t - (R_t + SP_t) - EL_t \quad (5)$$

where

S_{t-1} = Reservoir storage at the start of the period, t
S_t = Reservoir storage at the end of the period, t
I_t = Inflow during the period, t
R_t = Release for power generation during the period, t
El_t = Evaporation loss in the reservoir during the period, t
SP_t = Spill during the period, t

To calculate the evaporation loss, a linear relationship is established between the storage (S_t in Mm^3) and the corresponding water spread area (A_t in Mm^2) and is given by

$$A_t = 97.3064 + 0.0660426\ S_t, \quad (6)$$

evaporation Loss $EL_t = e_t * A_t$, (7)

where e_t is the depth of evaporation for the month t.

STORAGE BOUND EQUATION

The reservoir storage in any period should lie between maximum capacity and minimum capacity of the reservoir. That is

$$S_t \geq S_{\min}, \quad (8)$$

$$S_t \leq S_{\max}, \quad (9)$$

where S_{min} = Minimum storage in MCM,

and S_{max} = Maximum storage in MCM.

TURBINE CONSTRAINT

The hydropower production by the turbine in each month (t), should be less than or equal to the turbine capacity.

$$P_t \leq P_{\max}, \quad (10)$$

where P_{max} = Maximum power generating capacity in MW.

MINIMUM DOWN STREAM RELEASE CONSTRAINT

The release at any time periods should be greater than or equal to the minimum specified value.

$$R_t \geq R_{\min}, \quad (11)$$

where R_{min} = Minimum downstream release in MCM.

OBJECTIVE FUNCTION

The hydropower equation is a nonlinear function of the water released through the turbines, the net water head and the plant efficiency as follows:

$$P_t = f(H_t, R_t) = \eta K_t H_t R_t, \quad (12)$$

Objective function $TP = \sum_{t=1}^{t=n} P_t$, (13)

where H_t = Head available for hydropower generation corresponding to the storage at the beginning of the period. The expression for H_t in terms of initial storage (S_t) is given by

$$H_t = 2.97509 \times 10^{-19} \times S_t^5 - 1.22254 \times 10^{-14} \times S_t^4 + 2.02056 \times 10^{-10} \times S_t^3 - 1.76003 \times 10^{-6} \times S_t^2 + 0.0098812 \times S_t + 30.4553, \quad (14)$$

K_t = Conversion factor to convert discharges into hydropower,

η = Efficiency of the turbine.

For present study, average head at periods is taken for analysis, which is obtained by substituting average storage value in the above expression for head.

PSO MODEL FOR RESERVOIR OPERATIONAL STUDY

The problem of optimal operations involves determining decision policies (reservoir release, reservoir storage) that will optimise certain objectives subject to numerous constraints. The present case study aims to optimise total power generation from system and there in to arrive operational policy. Linear programming has been considered one of the most widely used techniques in reservoir operation planning problem, which can handle linear constraints effectively. Any reservoir operational problem must satisfy the mass balance of flows, which generally treated as a constraint in linear programming. Unlike linear programming, PSO need simulation model to handle such a mass balance equation. In the present study, storage is kept as a swarm and in every move on the search space, the position of swarm is updated, ie storage value is improved. The release for a period is calculated from the mass balance equation since initial and final storage values are obtained through optimisation and it is used to calculate the power that can be generated, if the resulted power value exceed the maximum capacity of the turbine units, the release excess to maximum capacity will be treated as spill from the system for that period. The storage to each month i for particle q is generated randomly as follow:

$$\begin{aligned}\text{storage}_i^q &= \text{Minimum storage} + \\ &\quad r * (\text{Maximum storage} - \text{Minimum storage}),\end{aligned} \tag{15}$$

where r is a random number between 0 and 1.

The initial velocity vector is calculated as follows

$$v_i^q(0) = storage_i^q + r * (Gstorage_i(0) - storage_i^q). \tag{16}$$

The computational flow of PSO technique to the present problem can be described in the following steps.

Step 1 (Initialisation): Set the time counter t = 0 and generate N particles randomly according to the equation, Each particles in the initial population is evaluated using the objective function (J), and global storage value (Gstorage) for each period is obtained from global best objective function (Gbest). The global best objective value is a maximum value obtained by comparing all the solutions.

Step 2 (Velocity Updating): The initial velocity is calculated as per equation (3) and velocity for remaining move is calculated according to the equation (2).

Step 3 (Time updating): Update the time counter t = t +1

Step 4 (Position updating): The position of particle is calculated as below:

$$storage_i^q(t+1) = storage_i^q(t) + v_i^q(t+1). \quad (17)$$

If a storage value violates upper and lower limits in any dimension, set its position at the proper limit.

Step 5 (individual best updating): Each particle is evaluated according its present position. If $J^q(t) < J^q(t-1)$, q = 1,…N, then update individual best as

$Lbest_i(t)=storage_i(t-1)$ and $J^q Lbest(t) = J^q(t-1)$ and go to step 6; else go to step 6.

Step 6 (Global best updating): Search for the maximum value among J^qLbest (t) and this value is assigned as Gbest,

Step 7 (Stopping criteria): If one of the stopping criteria is satisfied then stop; else go to step 2. The search can be terminated if one of the following criteria is satisfied: (a) the number of iterations since the last change of the best solution is greater than a pre-specified number or (b) the number of iterations reaches the maximum allowable number. In this study, second criterion is adopted as stopping criteria.

THE PSO IMPLEMENTATION

The proposed PSO based approach is implemented using Visual Basic 6.0 language and the developed software program is executed on a Pentium IV PC. Initially, few runs have been made with different values of the inertia weight. In our implementation, the inertia weights c_1 and c_2 is considered as 2 and 2 respectively. Fig. 2 shows the convergence of solution under the selection of various vales of inertia weights. For present study, in case of higher value of inertia weight, the search towards global solution is rather fast than lower inertia weights. Other parameters are selected as: number of particles N = 20, maximum number of iteration = 200.

RESULTS AND DISCUSSION

The objective of the present study is to assess the maximum power that can be generated from Indirasagar reservoir. The Indirasagar reservoir is proposed to generate hydropower and to meet the irrigation demand. In present study, only hydropower generation is considered for modelling, because the demand for irrigation is very meagre. To assess the potential of power generation from Indirasagar reservoir, three approaches are proposed with objective of maximizing

total power production from the system. In the first approach, the minimum down stream constraints are relaxed, ie minimum downstream flow should be greater than zero. In second approach, the minimum downstream value is prescribed for each water year. The minimum downstream value for each year is selected in such a way that the constraint for minimum release is not get violated at any periods. The minimum down stream water release is considered as 1000 million cum for each month. This value is reduced in a step of 100 million cum in case of minimum flow constraints do not satisfy for a particular year. In third approach, firm power value is set as an additional constraint to the optimisation model. Firm power is the power that can be generated for entire periods. The hydropower production by the turbine in each month, should be less than or equal to the turbine capacity, and also it should be greater than or equal to the firm power committed for that month. In approach three, the power production value is taken as a swarm and this is the main change made with reference to first two approaches. To evaluate the power production, the procedure first determines the power value for all the months through updating of particle positions, then the storage value for each months are determined without considering evaporation losses from mass balance equations. For these storage values, the simulation calculates evaporation losses and subsequently the corrected value of release and power production value is arrived by simulating backwards. The results of all three approaches are presented in Table 1.

From the historical data of 32 years, Chandreshwar (1987) identified critical periods by using moving average methods and mass curve analysis. The critical periods were identified to be from September 1950 to June 1953 and October 1964 to June 1967 encompassing ninety percent and cent percent dependable year respectively. Critical period is a period during which a reservoir goes from a full condition to an empty condition. Figure 3 and 6 shows the monthly flow variation for the critical periods encompassing 90 % and 100% dependable years. The third approach is applied for both the critical periods under the bound of firm power generation.

The optimisation is carried out by considering dead storage as the initial storage for all the water years. It reveals that when discharge is set to have a minimum value of zero, the total power production during that year gives higher value while comparing the results of other two approaches. The model takes the advantage of holding more water as storage, since it provides higher level of head. Releasing the water after building up of storage to higher elevation will give more power rather than by releasing water uniformly over the periods. As the objective of the problem is maximizing the total power production for a considered period, the approach one tries to achieve this at the cost of releasing more water after building up higher storage and therein meagre or no release is made for remaining periods. To satisfy

the minimum down stream flow and minimum required flow to run the turbine, it is necessary to give the lower bound for release. Setting up the higher value of release for all the periods will not be appropriate while the model is made to optimise every water year (12 months) independently. During the low flow periods, the higher quantity of water may not be available to release. Uncertainties in reservoir inflows and energy demand are much larger compared to those in the generation plants. Keeping this in view, the power is maximized for independently with feasible downstream release. The results of the approach 2 are tabulated in Table 1. The total power production for almost all the period is found marginally lesser than the results of approach one. The quantity of spill found through approach 2 is marginally higher than the first approach for some years. This spill quantity can be minimized by allowing model to run more iteration to explore the possibility of global solution. In the third approach, minimum power production is set as firm requirement and total power production is maximized.

It can be seen from the Table 1 that during the water years 4, 5, 6 and 32, plants can generate only 125 MW months which is equal to installed capacity of one unit. During the water years 18 and 19, the firm power of 45MW months and 90 MW months can be generated. Out of 32 years of historical data analysis, it is found that the reservoir is experiencing spill in 12 times during the months of August and September. The model shows more than 1000 Million cum of water goes as a spill in either months or in each months. The possible additional power of 190 MW months can be generated during these spill periods by installing two more units. Analysis of results is carried out by setting up the initial storage value as one-fourth of live storage plus dead storage. The results of the model show higher value of spill with no improvement in additional generation of firm power comparing when the results of model with initial storage are set to dead storage. The reservoir should be operated in such a way that the carryover storage for every year comes to dead storage. The water years 4,5,6 and 32 falls in the critical period encompassing 90% dependable year and water years 18 and 19 fall in the critical period encompassing 100% dependable year. The identified critical periods (Chandreshwar, 1987) comprises of 34 and 33 months for 90 % and 100 % dependable year respectively. To assess the potential of generating maximum possible firm power from the system during the critical periods, third approach is considered. The initial storage for the critical periods is taken corresponding to the maximum capacity of the reservoir. The firm power of 160 MW months and 85 MW months are obtained for 90% and 100% dependable years. Figure. 4 and 5 shows the monthly storage variation and optimal power generation for the critical period encompassing 90 % dependable year. Figure. 7 and 8 shows the monthly storage variation and optimal power generation

for the critical period encompassing 90 % dependable year. Though Indirasagar reservoir is a multipurpose reservoir, the hydropower generation is considered as a prime purpose. In such a hydro system, the function of the reservoir is to provide flow regulation, which is determined by the load requirements and by the total developed head. The results of approaches 2 and 3 are most promising than the approach 1 in maintaining minimum down stream flow. Maintenance of adequate flow to meet downstream requirements is a key aspect of the operational strategy. As Indirasagar reservoir is a storage reservoir plant capable of storing seasonal or yearly floods for hydropower generation during low flow season, the plant discharges may still fluctuate considerably on a daily basis. In this case, it is desirable to regulate the minimum flow and the rate of change in flow releases. The model based on weekly inflow will be more adaptable in developing operation policies. The variation storage for all 32 water years is prepared in a single plot (Fig. 9). It is found that the storage during the months of August, September, October, November and December builds up to the maximum capacity for most of the water years. These months give the advantage of getting higher head value for power generation. The storage starts to fall from the month of January to June. From the results of 32 years, the minimum, maximum storage values are selected for each month. The average storage value is found out by taking average value for all 32 years. A graph (Fig. 10) is plotted for minimum storage, average storage and maximum storage that are found out from the results of optimization model.

CONCLUSIONS

A particle swarm optimisation model has been developed and applied to assess the firm power and total power generation from Indirasagar resevoir. Three approaches are considered to maximize the total power production. When releasing an adequate flow to meet downstream requirements as a key aspect, the potential of generating firm power from the system becomes important for efficient operation of the reservoir. The results of approaches based on restriction to discharge provide the most promising in terms of integrating the environmental considerations into the operational regime of the hydro development and it is considered the most important mechanisms for mitigating adverse impacts and maximising positive benefits. For Indirasagar reservoir, it is found that the firm power of 160 MW months can be generated about 90% dependence and 85 MW months for 100 % dependence. Out of 32 years of historical data analysed, model shows that twelve years experiencing spill during the months of August and September. The quantity of spill exceeds more than 1000 MCM of water in either months or in each month. The possible additional power of 190 MW months can be generated during these spill periods by installing

two more additional units. It is found from the present study that the PSO shows the good performance in coupling simulation and optimisation process as a single module.

REFERENCES

Ahmed J. A and Sarma A.K., 2004, ”Genetic algorithm for optimal operating policy of a multipurpose reservoir”, Water resources management, Kluwer Academic publishers, 1-17.

Chandreshwar prasad, 1987, “Critical period analysis of Narmadasagar complex”, M.E. Thesis, Anna University, Chennai.

Gygier, J.C., and Stedinger, J.R. 1985, “Algorithms for optimising hydropower system operation”, Water Resources Research, 21(1), 1-10.

Huang S.J 2001, “Enhancement of hydroelectric generation scheduling using ant colony system based optimization approaches’, IEEE Transactions on Energy Conversion, 16(3),296-301.

Kennedy, J. and Eberhart, R.C 1995, “Particle swarm optimization”, Proceedings of IEEE International Conference on Neural Networks. Piscataway, NJ, IEEE service center, 1942-1948.

Labadie 2004, “Optimal operation of multi reservoir systems: State of the art review”, Journal of water resources planning and management, ASCE, 130(2),93-111.

Loucks, D.P., Stedinger, J.R., and Haith, D.A 1981, Water resources systems planning and analysis. Prentice-Hall Inc., Englewood Cliffs, N.J.

Ndiritu JG 2003, ”Reservoir system optimisation using a penalty approach and a multi-population genetic algorithm”, Water SA, 29(3), 2003.

Oliveira and Loucks 1997, ”Operating rules for Multireservoir systems”, Water Resources Research, 33(4), 839-852.

Shi Y, Eberhart RC. Amodi.ed 1998 Particle swarm optimiser. In: Proceedings of the IEEE International Conference on Evolutionary Computation. Piscataway NJ: IEEE Press, 69–73.

Simonovic 1992, “Reservoir systems analysis: closing gap between theory and practice”, Journal of water resources planning and management, ASCE, 118(3), 262-280.

Stedinger, J.R., Sule, B.F., and Loucks, D.P. 1984, “Stochastic dynamic programming models for reservoir operation optimisation” Water Resources Research, 20(11), 1499-1505.

Tejada-Guibert, J.A., Johnson, s.A., and Stedinger, J.R. 1995, “ The value of hydrologic information in stochastic dynamic programming models of a multireservoir system,” Water Resources Research, 31(10), 2571-2579.

Wardlaw, R and Sharif, M 1999, “Evaluation of genetic algorithms for optimal reservoir system operation”, Journal Water Resources planning and management, ASCE, 125(1), 25-33.

Yeh, W. 1985, “Reservoir management and operations models: A state of the art review”, Water Resources Research, 21(12), 1797-1818.

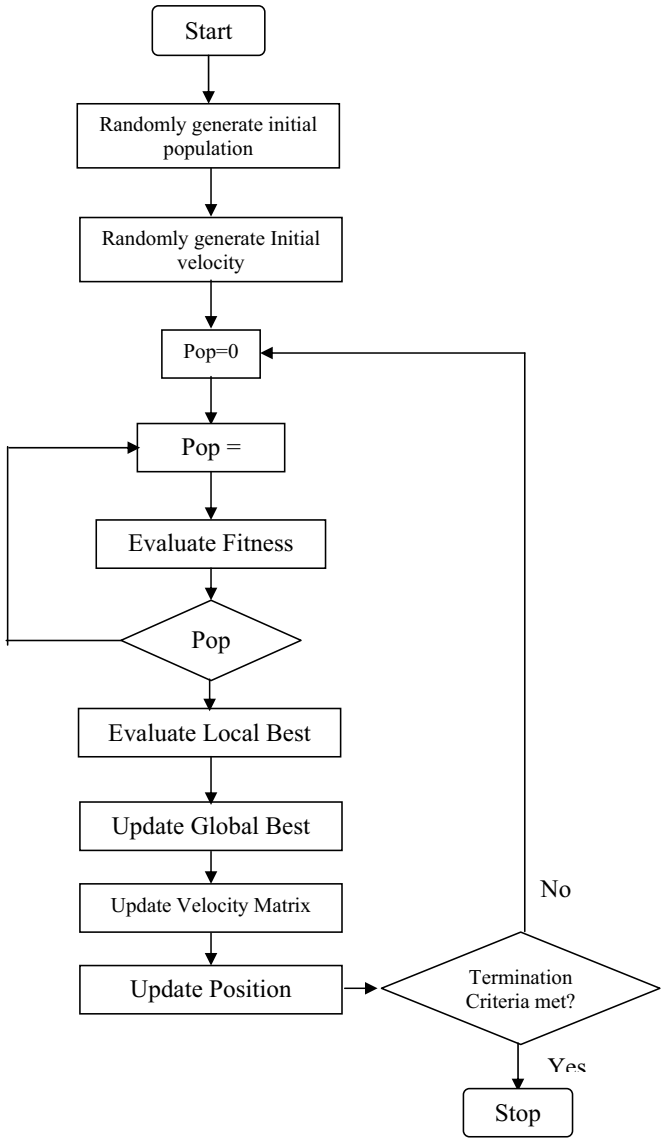

Fig. 1 Flow chart of particle swarm algorithm

Table 1. Particle Swarm Optimisation results for three approaches

	Approach 1		Approach 2			Approach 3		
Water Year	Total Power (MW year)	Spill (Million cubic metre)	Min Release	Total Power (MW year)	Spill (Million cubic metre)	Firm Power (MW month)	Total Power (MW year)	Spill (Million cubic metre)
1	7134	1083	1000	7039	2391	270	7161	1084
2	5788	-	1000	5588	-	250	5602	-
3	5498	-	700	5474	13	200	5533	10.4
4	2588	-	500	2229	-	125	2220	-
5	4246	-	600	3798	-	125	3879	-
6	4156	-	700	3765	-	125	3794	-
7	4961	-	800	4832	-	200	4826	-
8	7027	1277	500	6938	1812	180	7036	1324
9	7734	4122	1000	7721	4122	402	7733	4122
10	3555	-	600	3180	-	175	3168	-
11	5063	-	1000	4864	-	300	4766	-
12	7068	10668	1000	7064	10666	325	7061	10668
13	5502	-	1000	5441	-	250	5510	-
14	8059	20556	1000	8046	20567	350	8053	20556
15	4426	-	900	4283	-	200	4310	-
16	4286	-	400	3987	-	175	2954	-
17	5784	10.8	800	5722	-	200	5746	21.1
18	1788	-	200	1086	-	45	1090	-
19	2588	-	300	2055	-	90	2047	-
20	5239	-	750	5137	-	230	5149	11
21	4320	-	700	3925	-	175	3937	-
22	6324	3239	1000	6130	4308	325	6290	3300.5
23	6884	2202	1000	6582	3766	380	3843	2209
24	6400	-	600	6354	6.4	250	6433	15.80
25	4914	-	1000	4664	-	200	4732	-
26	6268	10330	1000	6290	10330	325	6287	10330
27	3801	-	600	3643	-	175	3576	-
28	6644	4562	1000	6498	5715	250	6661	4566
29	5044	-	700	4826	-	300	3893	-
30	8206	4477	1000	8092	5691	485	8210	4477
31	7627	2197	1000	7627	2198	450	7585	2198
32	3032	-	1000	2673		125	2674	-

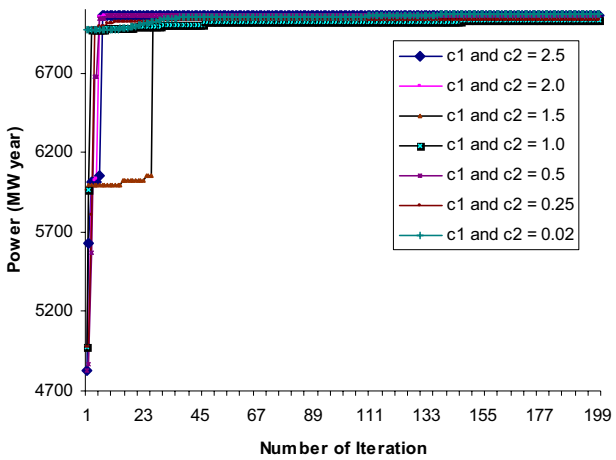

Fig. 2 Convergence of solution

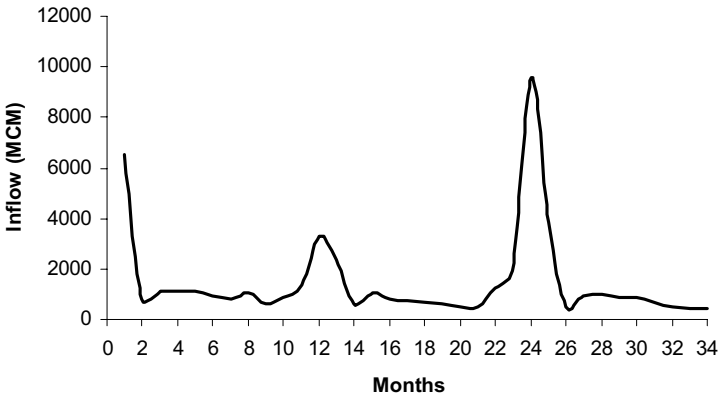

Fig. 3 Monthly flow variation for critical period encompassing 90 % dependable year

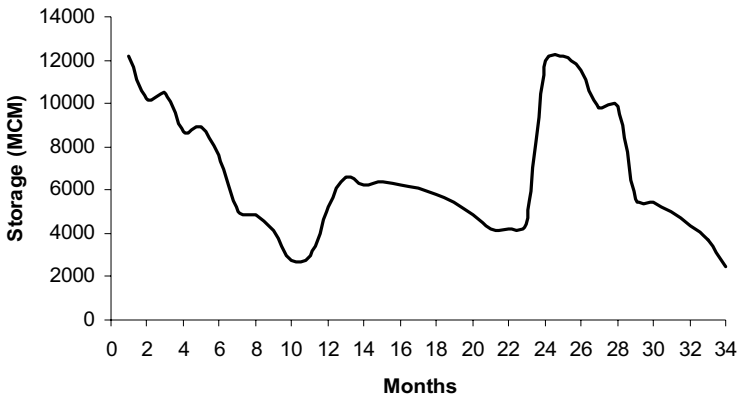

Fig. 4 Monthly storage variation for Critical period encompassing 90 % dependable year

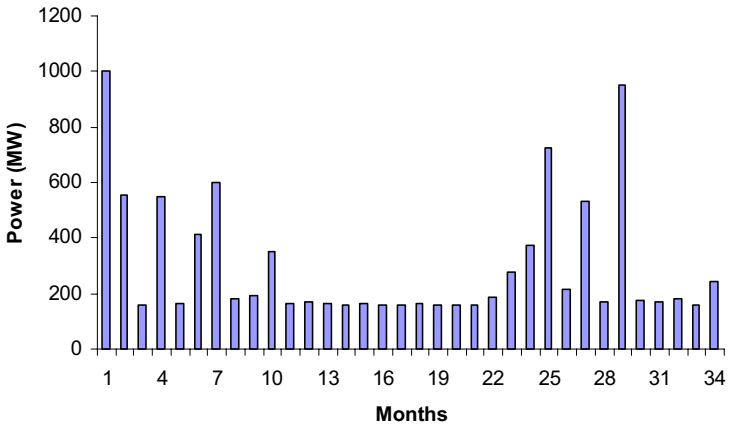

Fig. 5 Optimal Power generation for critical period encompassing 90 % dependable year

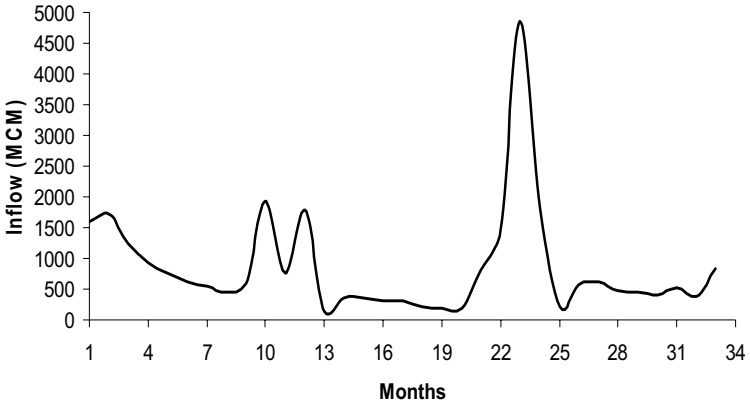

Fig. 6 Monthly flow variation for critical period encompassing 100 % dependable year

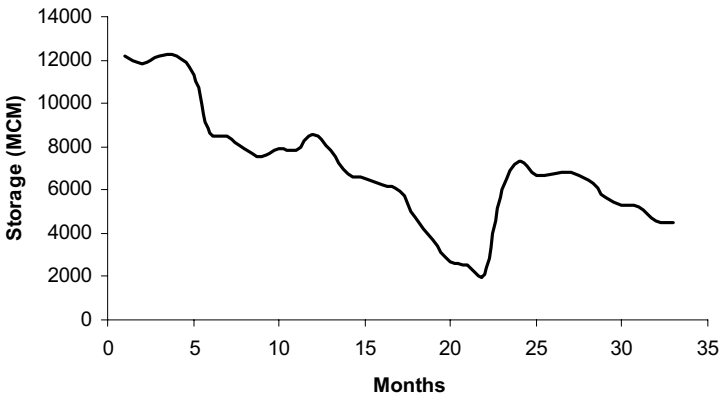

Fig. 7 Monthly storage variation for critical period encompassing 100 % dependable year

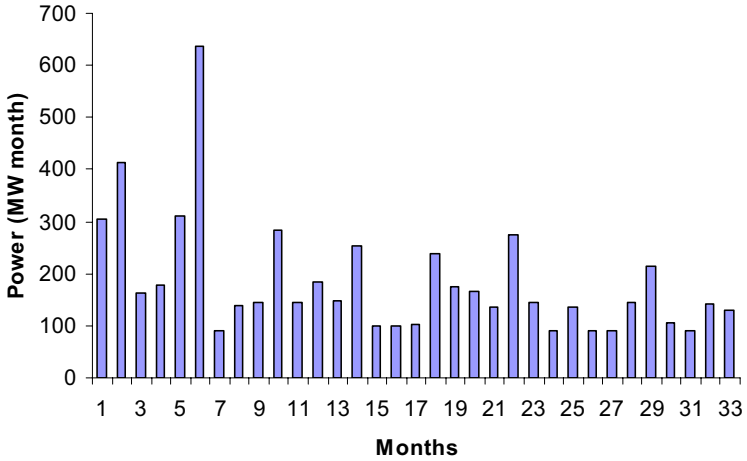

Fig. 8 Optimal power generation for critical period encompassing 100 % dependable year

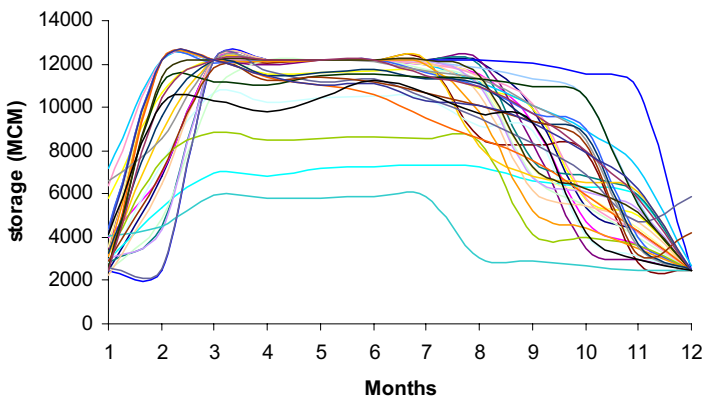

Fig. 9 Plot showing the variation of storage for historical water years

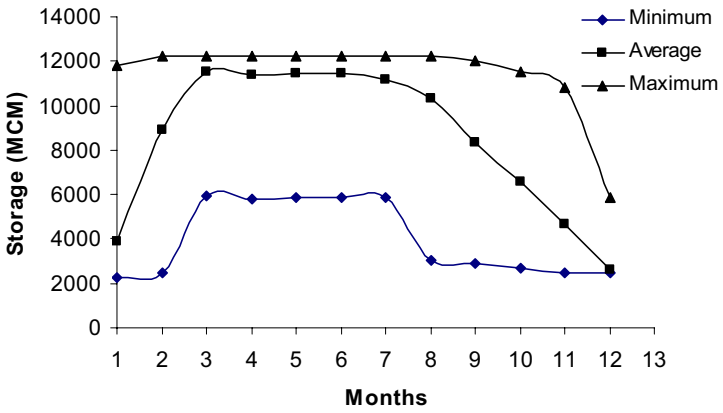

Fig. 10 Monthly storage variation for optimal operation

Submission of Manuscripts

International Journal of Ecology & Development (IJED)

ISSN 0972-9984

The authors should submit two complete hard copies of manuscript of their unpublished and original paper (with an electronic copy) to *Editor-in-Chief, International Journal of Ecology & Development (IJED), Indian Society for Development & Environment Research, Post Box No. 113, Roorkee-247667, INDIA*; **Email:** *ijed@isder.ceser.res.in*. It will be assume that authors will keep a copy of their paper. We strongly encourage electronic submission of manuscript by email along with one hard copy.

Format of Manuscripts:

Please send your paper as a single document including tables and figures. This means, it should be one Microsoft Word file ... AND NOT a zipped File containing different files for text, tables, figures, etc. The paper should not normally exceed 5000 words, and should conform to the following:

- Cover page giving title, author(s), affiliation(s), mailing address and e-mail address
- All pages should be without page number, header Text and footer text.
- Abstract describing the context and scope of the paper
- Keywords
- JEL/ MSC Subject Classification
- Main text
- References

The manuscript should be as ***MS Word*** or ***PDF*** **file** in the following format-

Page Size	**A4** (8.27" x 11.69") **without page number**
Page Margin	Top=1.0 inch, Bottom=1.0 inch Left=1.25", Right=1.25"
Font Face	Times New Roman
Font Size for Title	18 pt. Bold & Title Case
Font Size for Headings	12 pt. Bold & CAPITAL CASE
Font Size for Sub-Headings	12 pt. Bold & Title Case
Alignment for Title & Headings	Center
Font size for Text	12 pt.
Line Space for Text	1.5 line space
Paragraph	No Tab, and 12 pt. Space after paragraph & Alignment=Justify
Abstract & Keyword	Margin: Top=1.5 inch, Left=1.5 inch, Font: size=10 pt. Font Face =Arial & italic Align= justify Line Space=single
Reference	Align= justify Line Space=single and 10 pt. space before the next reference.
Table and Figures	Should be separate and at the last of manuscript. Line space=single

Submission of a paper implies that the reported work is neither under consideration for a scientific journal nor already published. All manuscripts are subject to peer review. If revisions are required for acceptance of a manuscript, one copy of the revised manuscript should be submitted. Print copy of the journal will be dispatch to subscribers only. However, authors will get the e-issue of journal without any payment. A free print (paper) issue of journal will be available to the authors whose institutions subscribe. A copy of single issue of journal is available on a special discount to the authors only. Furthermore, you are welcome to support the journal by requesting that your library to subscribe the journal, or by taking out an individual subscription.

Preparation of the Manuscript

Papers must be clearly written in English. All sections of the manuscript should be typed, double-spaced, on one side of the paper only. In addition to the full title of the paper, authors should supply a running title, of less than 40 characters, and up to five keywords.

Research papers should be accompanied by an abstract, which will appear in front of the main body of the text. It should be written in complete sentences and should summarize the aims, methods, results and conclusions in less than 250 words. The abstract should be comprehensible to readers before they read the paper, and abbreviations and citations should be avoided.

Authors are responsible for the accuracy of references. Within the text, references should be cited by author's name(s) and year of publication (where there are more than two authors please use et al.). Published articles and those in press (state the journal which has accepted them and enclose a copy of the manuscript) may be included. Citations should be typed at the end of the manuscript in alphabetical order, with authors' surnames and initials inverted. References should include, in the following order: authors' names, year, paper title, journal title, volume number, issue number, inclusive page numbers and (for books only) name and address of publishers. References should therefore be listed as follows:

> Natterer, F., 1986, *The Mathematics of Computerized Tomography,* John Wiley & Sons, New York.
>
> Herman, G.T., 1972, Two *Direct Methods for Reconstructing Pictures from their Projections: A Comparative Study,* Computer Graphics and Image Processing, 1, 123-144.
>
> Natterer, F., 1997, *An Algorithm for 3D Ultrasound Tomography*, in G. Chavent and P.C. Sabatier (eds.): *Inverse Problems of Wave Propagation and Diffraction*. Springer, New York.
>
> Gordon, R., Bender, R. and Herman G. T., 1970, Algebraic Reconstruction Techniques (ART) for Three Dimensional Electron Microscopy and X-Ray Photography, J. Theoret. Biol. 29, 471-481.

Tables should be self-explanatory and should include a brief descriptive title. Illustrations should be clearly lettered and of the highest quality. Acknowledgements and Footnotes should be included at the end of the text. Any footnote should be identified by superscripted numbers.

SUBSCRIPTIONS

International Journal of Ecology & Development (IJED)

ISSN 0972-9984

Followings are the Annual Subscription rate for year 2006 (for a volume):

Issues	Individual	Library
Print Issue:	**Euro/US$ 350.00**	**Euro/US$ 450.00**
Online:	**Euro/US$ 300.00**	**Euro/US$ 450.00**
Print Issue and Online (Both):	**Euro/US$ 450.00**	**Euro/US$ 650.**

Subscriptions in India ? Please subtract Euro/US$ 30.00 for print issue (postage+handling charges).

How to Pay Subscriptions?

Subscriptions are payable in advance. Subscribers are requested to send payment with their order. Issues will only be sent on receipt of payment. Subscriptions are entered on an annual basis and may be paid in Rupees or US Dollars/Euro.

Payment can be made by Bank Draft/ Bank Wire Transfers/ Bank Cheque (please add US $/Euro 25 as cheque transfer charges, in case of cheque) only. *All payments should be send to "*Indian Society for Development & Environment Research"*, Post Box No. 113, Roorkee-247667, INDIA".* The bank draft should be drawn on Roorkee, India.

Claims and Cancellations

Claims for issues not received should be made in writing within three months of the date of publication. Cancellations: no refunds will be made after the first issue of the journal for the year has been dispatched.

Detailed information and instructions are available at

Http://www.isder.ceser.res.in/ijed.html